cmgh
CELLULAR AND MOLECULAR GASTROENTEROLOGY AND HEPATOLOGY

ORIGINAL RESEARCH

Pancreatic Ductal Deletion of *Hnf1b* Disrupts Exocrine Homeostasis, Leads to Pancreatitis, and Facilitates Tumorigenesis

Evans Quilichini,[1] Mélanie Fabre,[1] Thassadite Dirami,[1] Aline Stedman,[1] Matias De Vas,[1] Ozge Ozguc,[1] Raymond C. Pasek,[2] Silvia Cereghini,[1] Lucie Morillon,[1] Carmen Guerra,[3] Anne Couvelard,[4] Maureen Gannon,[2] and Cécile Haumaitre[1]

[1]*UMR7622 Sorbonne Université, Centre National de la Recherche Scientifique, Institut de Biologie Paris-Seine, Paris, France;* [2]*Department of Medicine, Vanderbilt University Medical Center, Nashville, Tennessee;* [3]*Molecular Oncology Program, Centro Nacional de Investigaciones Oncológicas, Madrid, Spain;* [4]*Hôpital Bichat, Département de Pathologie, Assistance Publique-Hôpitaux de Paris, Université Paris Diderot, Paris, France*

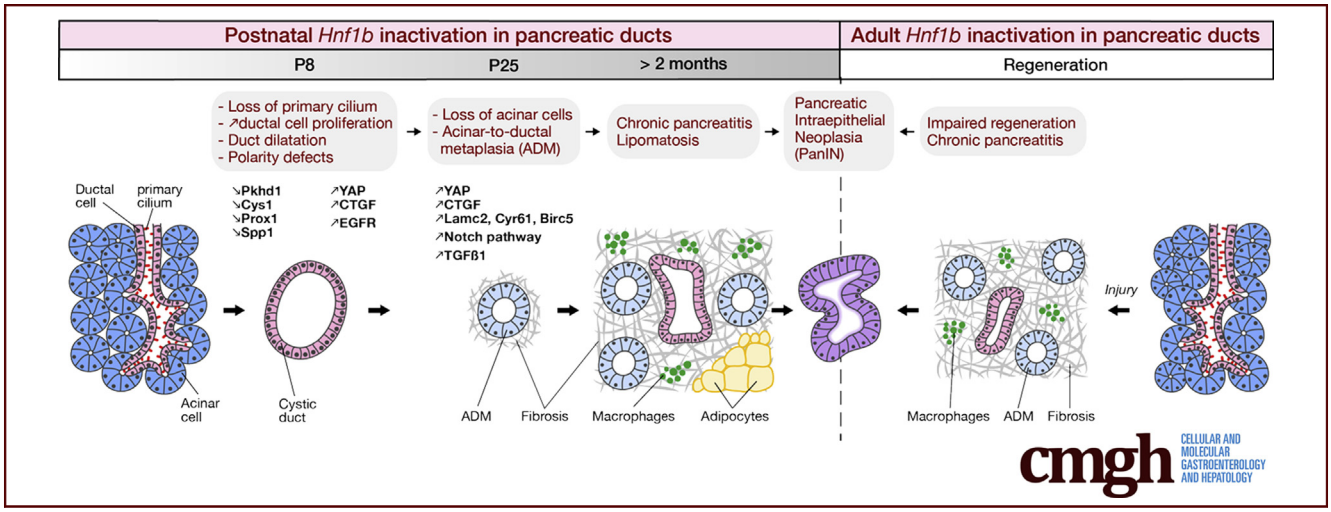

SUMMARY

This study shows how *Hnf1b* inactivation in pancreatic ductal cells leads to chronic pancreatitis, neoplasia, and potentiates pancreatic intraepithelial neoplasia formation. This shows a cause of pancreatitis and identifies Hnf1b as a potential tumor suppressor for pancreatic cancer.

BACKGROUND & AIMS: The exocrine pancreas consists of acinar cells that produce digestive enzymes transported to the intestine through a branched ductal epithelium. Chronic pancreatitis is characterized by progressive inflammation, fibrosis, and loss of acinar tissue. These changes of the exocrine tissue are risk factors for pancreatic cancer. The cause of chronic pancreatitis cannot be identified in one quarter of patients. Here, we investigated how duct dysfunction could contribute to pancreatitis development.

METHODS: The transcription factor Hnf1b, first expressed in pancreatic progenitors, is strictly restricted to ductal cells from late embryogenesis. We previously showed that Hnf1b is crucial for pancreas morphogenesis but its postnatal role still remains unelucidated. To investigate the role of pancreatic ducts in exocrine homeostasis, we inactivated the *Hnf1b* gene in vivo in mouse ductal cells.

RESULTS: We uncovered that postnatal *Hnf1b* inactivation in pancreatic ducts leads to chronic pancreatitis in adults. *Hnf1b*Δ^{duct} mutants show dilatation of ducts, loss of acinar cells, acinar-to-ductal metaplasia, and lipomatosis. We deciphered the early events involved, with down-regulation of cystic disease–associated genes, loss of primary cilia, up-regulation of signaling pathways, especially the Yap pathway, which is involved in acinar-to-ductal metaplasia. Remarkably, *Hnf1b*Δ^{duct} mutants developed pancreatic intraepithelial neoplasia and promote pancreatic intraepithelial neoplasia progression in concert with KRAS. We further showed that adult *Hnf1b* inactivation in pancreatic ducts is associated with impaired regeneration after injury, with persistent metaplasia and initiation of neoplasia.

CONCLUSIONS: Loss of *Hnf1b* in ductal cells leads to chronic pancreatitis and neoplasia. This study shows that Hnf1b deficiency may contribute to diseases of the exocrine pancreas and gains further insight into the etiology of pancreatitis and tumorigenesis. *(Cell Mol Gastroenterol Hepatol 2019;8:487–511; https://doi.org/10.1016/j.jcmgh.2019.06.005)*

Keywords: Pancreatitis; Pancreatic Cancer; Hnf1b; Ducts; Acinar-to-Ductal-Metaplasia.

Pancreatitis is a common disorder with significant morbidity and mortality, yet little is known about its pathogenesis, and there is no specific or effective treatment. It is characterized by progressive inflammation, necrosis/apoptosis, fibrosis, loss of acinar tissue and acinar-to-ductal metaplasia (ADM). Chronic pancreatitis increases the risk of pancreatic cancer.[1] Pancreatic ductal adenocarcinoma (PDAC) is one of the most lethal malignancies in human beings, occurring through the progression of precursor lesions, the best described being pancreatic intraepithelial neoplasia (PanIN). ADM is critical in neoplastic transformation because metaplastic acinar cells can undergo the reprogramming process from ADM to form PanINs.[2,3] Fibrosis also provides the background for PanIN development.[4]

The major etiologies of pancreatitis are obstruction of the pancreatic duct, usually caused by gallstones, alcohol, and smoking. Pancreatitis also has been associated with genetic factors, including mutations of the *CFTR* gene, as well as *Protease serine 1 (PRSS1), Serine Protease Inhibitor Kazal Type 1 (SPINK1), Chymotrypsin C (CTRC),* and *Claudin 2 (CLDN2) genes*. However, the cause of chronic pancreatitis cannot be identified in approximately 30% of patients.[4]

The exocrine compartment of the pancreas consists of acinar cells that secrete enzymes and an intricate system of epithelial ductal cells that secrete the fluid carrying the digestive enzymes in the gut. Ductal cells comprise centroacinar cells and intercalated intralobular and interlobular ducts, linking the acinar lobules to the main pancreatic duct that drains into the duodenum.[5] In vertebrates, pancreatic duct morphogenesis initiates with the formation of a network of primitive ducts, which matures into a tubular system. A restricted set of transcription factors are involved in ductal cell differentiation such as Sox9 and Hnf1b.[5,6] Although acinar cells are not ciliated, ductal cells harbor an immotile primary cilium.[7–9] These microtubule-based organelles projecting from the surface of the pancreatic ductal cells function as chemosensors and mechanosensors, and integrate multiple signaling pathways.[10] Except for duct obstruction and mutations in the *CFTR* gene, duct contribution in acinar cell homeostasis is poorly known and the cellular and molecular mechanisms leading to acinar damage and chronic pancreatitis are poorly understood.

In the present study, we investigate how duct dysfunction may contribute to pancreatitis. We focused on the transcription factor Hnf1b, which presents a very interesting profile. It is first expressed in pancreatic progenitors, then restricted to ductal cells from late embryogenesis such as only few transcription factors, and therefore not expressed in acinar cells.[11–13] We previously showed that Hnf1b is crucial for duct morphogenesis during embryogenesis.[13] Here, we investigate its role in differentiated ducts after birth. In the postnatal pancreas, acinar cells do not derive from ducts,[12,14,15] allowing analysis of the role of Hnf1b in duct function and the consequences on acinar cell homeostasis.

Our data show that Hnf1b has a crucial function in the regulatory network controlling differentiated epithelial ductal cells and maintenance of the primary cilium. Its ductal function is critical to maintain acinar homeostasis because loss of Hnf1b in ductal cells leads to chronic pancreatitis and neoplasia. Thus, *Hnf1b* deficiency causes dysfunction of the exocrine pancreas, providing further insights into the etiology of pancreatitis and a risk factor for tumorigenesis.

Results

Postnatal Inactivation of Hnf1b in Pancreatic Ducts Leads to Loss of Primary Cilia and Cystic Duct Formation

To perform a postnatal conditional inactivation of *Hnf1b* in ductal cells, we generated Sox9-CreER;Hnf1b$^{fl/fl}$;R26R^{YFP} mutants and conditionally inactivated *Hnf1b* during the first 3 days after birth (postnatal day [P] P1–P3), further mentioned as *Hnf1b*Δ^{duct} mutants. We analyzed the consequences on pancreata dissected 5 days after the last tamoxifen (TM) injection, at P8. We assessed that *Hnf1b* inactivation in pancreatic ductal cells was efficient by reverse transcription-quantitative polymerase chain reaction (RT-qPCR), showing a 65% decrease in *Hnf1b* expression in mutants (Figure 1*A*). By immunostaining, we observed nuclear Hnf1b localization in ductal structures in controls (Figure 1*B* and *C*), whereas Hnf1b was absent from green fluorescent protein (GFP) positive ducts in mutants. Hnf1b protein persisted in only 14% of nonrecombined ducts, negative for GFP (Figure 1*D*).

As a transcription factor, Hnf1b controls a network of genes involved in duct morphogenesis during development.[13] To investigate the role of *Hnf1b* in differentiated ducts after birth, we analyzed the expression of genes involved in the maintenance of the primary cilium and in ductal cell integrity and functionality (Figure 1*E*). In *Hnf1b*Δ^{duct} mutants, we found a significant decrease in expression of cystic disease genes by RT-qPCR, known as direct targets of Hnf1b in renal cells or in pancreatic progenitors.[13–17] We observed a strong decrease in *Pkhd1*, *Cys1*, *Spp1*, and *Prox1* expression, involved in ciliary maintenance and/or tubular architecture.[18–21] *Tg737/Ift88* required for ciliogenesis also was down-regulated significantly. By contrast, the expression of the ductal markers *Sox9*, *Hnf6*, and *Ck19* was unchanged compared with controls, showing that ductal cell differentiation is maintained. Moreover, expression of *Cftr* was unaffected in *Hnf1b*Δ^{duct} mutants.

Because we found a specific down-regulation of genes involved in the maintenance of the ductal primary cilium, we

Abbreviations used in this paper: **ADM, acinar-to-ductal metaplasia; CTGF, connective tissue growth factor; D, day; E, embryonic; EGFR, epidermal growth factor receptor; EMT, epithelial-mesenchymal transition; GFP, green fluorescent protein; P, postnatal; PanIN, pancreatic intraepithelial neoplasia; PBS, phosphate-buffered saline; PDAC, pancreatic ductal adenocarcinoma; PPH3, phospho-histone H3; PSC, pancreatic stellate cell; RT-qPCR, reverse-transcription quantitative polymerase chain reaction; α-SMA, α-smooth muscle actin; TGF, transforming growth factor; TM, tamoxifen; TUNEL, terminal deoxynucleotidyl transferase–mediated deoxyuridine triphosphate nick-end labeling.**

Most current article

© 2019 The Authors. Published by Elsevier Inc. on behalf of the AGA Institute. This is an open access article under the CC BY-NC-ND license (http://creativecommons.org/licenses/by-nc-nd/4.0/).

2352-345X
https://doi.org/10.1016/j.jcmgh.2019.06.005

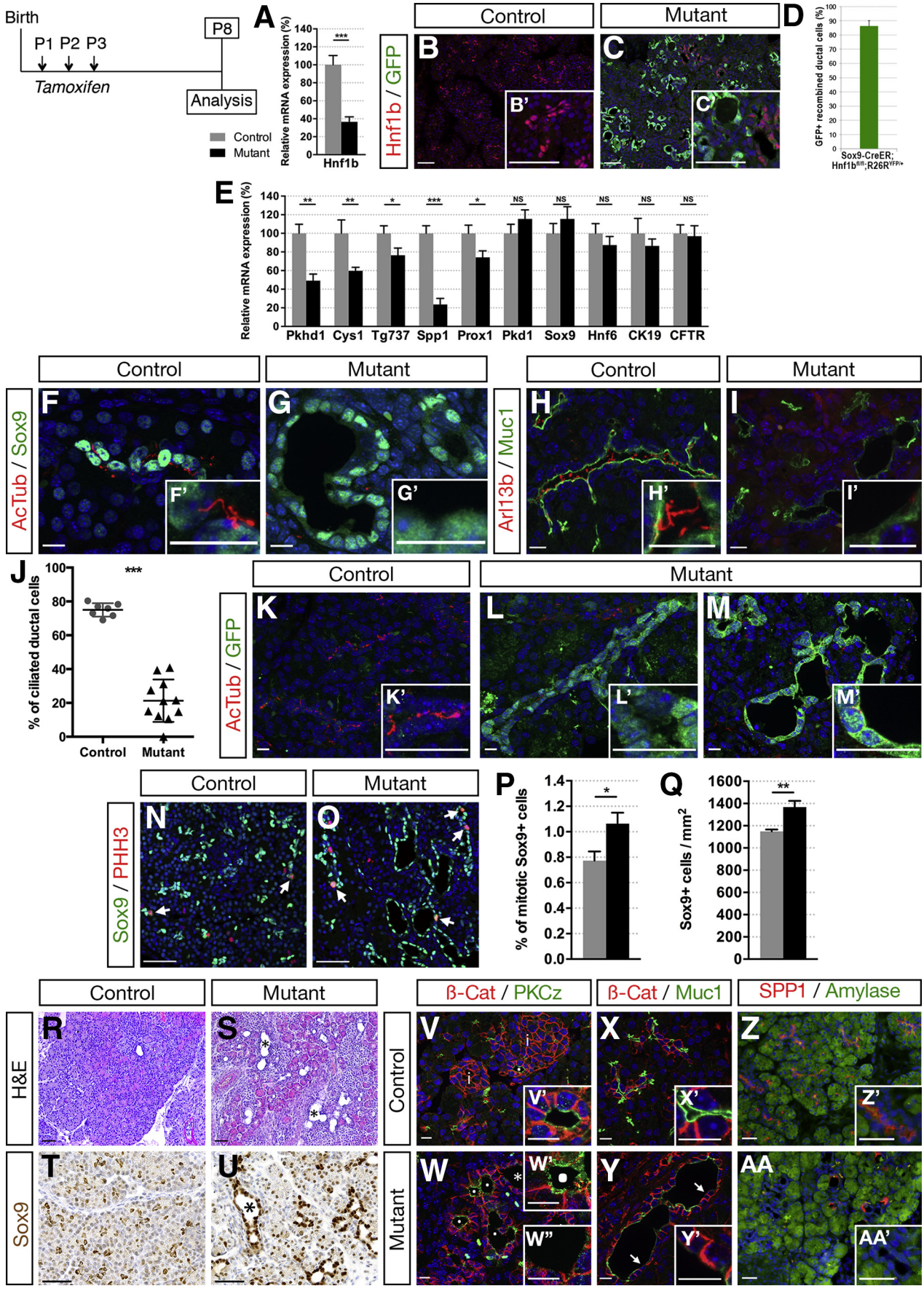
Birth
P1 P2 P3
Tamoxifen
P8
Analysis
A
Relative mRNA expression (%)
Hnf1b
Control
Mutant
Hnf1b / GFP
B
B'
C
C'
D
GFP+ recombined ductal cells (%)
Sox9-CreER; Hnf1b fl/fl; R26R YFP/+
E
Relative mRNA expression (%)
Pkhd1
Cys1
Tg737
Spp1
Prox1
Pkd1
Sox9
Hnf6
CK19
CFTR
AcTub / Sox9
F
F'
G
G'
Arl13b / Muc1
H
H'
I
I'
J
% of ciliated ductal cells
Control
Mutant
AcTub / GFP
K
K'
L
L'
M
M'
Sox9 / PHH3
N
O
P
% of mitotic Sox9+ cells
Q
Sox9+ cells / mm2
H&E
R
S
Sox9
T
U
ß-Cat / PKCz
ß-Cat / Muc1
SPP1 / Amylase
V
V'
X
X'
Z
Z'
W
W'
W"
Y
Y'
AA
AA'

examined primary cilia in *Hnf1b*Δ^{duct} mutants. Immunostaining of acetylated α-tubulin, a tubulin modification present on primary cilium axonemes, showed a loss of cilia in ductal cells of *Hnf1b*Δ^{duct} mutants (Figure 1*F* and *G*). This was confirmed by the absence of Arl13b immunostaining, a cilium-specific membrane protein (Figure 1*H* and *I*). Quantification showed a 73% decrease in ciliated ductal cells in *Hnf1b*Δ^{duct} mutants (Figure 1*J*), in agreement with the level of *Hnf1b* inactivation efficiency. To correlate *Hnf1b* inactivation and the loss of the primary cilium at the cellular level, we performed acetylated α-tubulin/GFP co-immunostainings. *Hnf1b*-inactivated ducts labeled with GFP do not present any cilia (Figure 1*K–M*).

Because loss of cilia may promote aberrant cell division, permitting increased proliferation,[22] we quantified proliferation of ductal cells by Sox9/Phospho-histone H3 (PPH3) immunostainings (Figure 1*N* and *O*). Mutant ducts presented more proliferative cells than control pancreatic ducts (1.4-fold) (Figure 1*P*). This resulted in a significant increase of the ductal cell area (1.2-fold), quantified by the number of Sox9+ cells (Figure 1*Q*).

We investigated if these abnormalities could lead to cyst formation. By H&E staining, we observed dilated ducts in *Hnf1b*Δ^{duct} mutants (Figure 1*R* and *S*). Sox9 and Hnf6 showed nuclear staining of enlarged mutant ductal structures (Figure 1*T* and *U*, and data not shown), showing that dilated ducts still express some terminal differentiation markers. We further analyzed ductal cell polarity. Control ducts showed strong apical localization of Muc1 and Protein kinase C zeta in epithelial cells around the duct lumen (Figure 1*V–Y*). In *Hnf1b*Δ^{duct} mutants, this apical staining persisted in nondilated ducts (Figure 1*W'*), whereas it was reduced and discontinuous in the cells lining cysts in mutants (Figure 1*W''*). Although the Spp1/osteopontin matricellular protein was localized on the apical side of control ductal cells, we observed very few Spp1+ cells in mutants, confirming RT-qPCR results (Figure 1*Z* and *AA*).

Altogether, these results show that Hnf1b has a prominent role in the regulatory network controlling the maintenance of the primary cilium and tubular architecture of pancreatic ducts after birth.

Postnatal Inactivation of Hnf1b in Pancreatic Ducts Leads to Non–Cell Autonomous Effects on Acinar Cells Through Activation of the YAP Mechanotransducer

A direct antagonistic interaction between ciliogenesis and YAP function has been shown.[23] YAP activation also was observed in hepatic cystogenesis associated with *Pkhd1* deficiency.[24] YAP has a central role as a mechanoeffector and sensor of cell polarity, being a mediator of mechanical cues and linking the physicality of cells and tissues to potent transcriptional responses. It is mechanically regulated by various regimens of cell stretching, such as deformations of epithelial monolayers.[25–27] In *Hnf1b*Δ^{duct} mutants, we visualized the deformation of pericystic areas with immunostaining of the fibroblast marker α-smooth muscle actin (α-SMA) at P8. Although α-SMA+ cells were restricted around blood vessels in control pancreata (Figure 2*A*), mutants displayed widespread α-SMA staining showing activation of fibroblasts surrounding ducts and in periacinar spaces (Figure 2*A* and *B*). Interestingly, we observed an increased number of cells with YAP nuclear staining in *Hnf1b*Δ^{duct} mutants in pericystic and acinar areas (Figure 2*C–F*). Consistent with YAP activation, we found a strong increase in YAP transcriptional targets, with up-regulation of *Ctgf* (1.8-fold) and *Lamc2* in *Hnf1b*Δ^{duct} mutants compared with controls (Figure 2*G*). To determine in which cell type we observed the YAP nuclear enrichment, we performed co-immunostainings for YAP/Sox9 and YAP/amylase to analyze ductal and acinar cells, respectively. Although in controls YAP localized only in the nucleus of Sox9+ ductal cells (Figure 2*H–M*), in mutants, it also localized ectopically in amylase+ acinar cells (Figure 2*N–S*), suggesting that mechanical stress induced by enlarging cysts stimulates YAP activation in acinar cells at P8. These data show cell autonomous and non–cell autonomous up-regulation of the YAP pathway when *Hnf1b* is inactivated in ductal cells.

Postnatal Inactivation of Hnf1b in Ducts Leads to ADM, Loss of Acinar Cells, and Lipomatosis

YAP nuclear localization and increased expression of the YAP target gene *Ctgf* is particularly interesting because of its

Figure 1. (***See previous page***). **Ductal deletion of *Hnf1b* leads to loss of primary cilia, increased ductal cell proliferation, dilatation, and alteration of ductal cell polarity at P8.** (*A*) Analysis of *Hnf1b* inactivation efficiency by RT-qPCR. (*B* and *C*) Hnf1b (red) and GFP (green) immunostaining. Hnf1b+ ductal cells are observed in controls and recombination is monitored by GFP+ cells in Sox9-Cre^{ER};Hnf1b$^{fl/fl}$;R26R$^{YFP/+}$ mutant pancreata. (*D*) Quantification of GFP+ recombined ductal cells in Sox9-Cre^{ER};Hnf1b$^{fl/fl}$;R26R$^{YFP/+}$ mutant pancreata. (*E*) RT-qPCR of ductal and cystic-disease genes. (*F* and *G*) Sox9 (green) and acetylated α-tubulin (Ac-Tub, red) immunostaining. (*H* and *I*) Muc1 (green) and Arl13b (red) immunostaining. Mutant ductal epithelial cells stained with Sox9 and Muc1 are devoid of primary cilia, stained for (*G'*) Ac-Tub and (*I'*) Arl13b. (*J*) Quantification of ciliated ductal cells. (*K–M*) GFP and Ac-Tub immunostaining showing primary cilia loss in recombinant ductal cells from (*M'*) dilated and (*L'*) nondilated ducts. (*N* and *O*) Phospho-histone H3 (PHH3, red) and Sox9 (green) immunostaining. (*P* and *Q*) Quantification of ductal Sox9^{+} cell proliferation and quantification of the number Sox9^{+} cells per area. *Arrows* indicate mitotic Sox9^{+} cells. (*R* and *S*) H&E staining. (*T* and *U*) Sox9 (brown) immunohistochemistry. (*V* and *W*) Protein kinase C zeta (green) and β-catenin (red) immunostaining. (*W*) *Asterisk* shows dilated duct with loss of Protein kinase C zeta apical staining. Protein kinase C zeta apical staining is maintained in (*W'*) nondilated duct, but lost in (*W''*) dilated ducts. (*X* and *Y*) Mucin1 (Muc1, green) and β-catenin (β-Cat, red) immunostaining. (*Y* and *Y'*) *Arrows* show disruption of Muc1 staining in parts of mutant dilated ducts. (*Z* and *AA*) Spp1 (red) and amylase (green) immunostaining. Loss of the apical ductal marker Spp1 was observed in mutants (*AA'*). Nuclei are stained with 4′,6-diamidino-2-phenylindole (blue). *Scale bars*: (*B*, *C*, *N*, *O*, and *R–U*) 50 μm; (*X* and *Y*) 30 μm; (*F–I*, *K–M*, *V*, *W*, *Z*, and *AA*) 10 μm. Control, n = 7; mutant, n = 7 for RT-qPCR; and control, n ≥ 3; mutant, n ≥ 3 for immunostainings. *$P < .05$; **$P < .01$; ***$P < .001$. mRNA, messenger RNA.

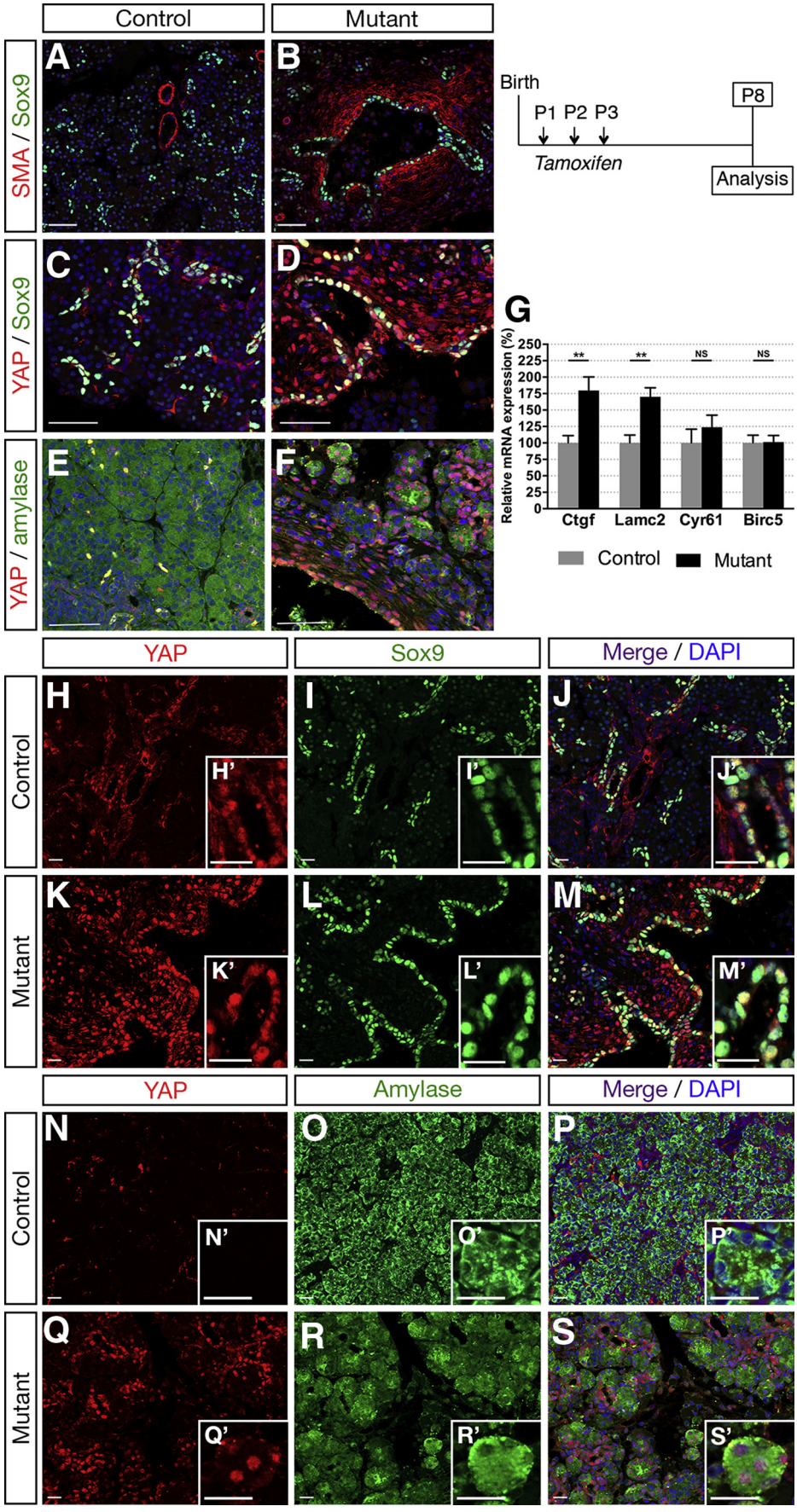

Figure 2. Ductal deletion of *Hnf1b* leads to up-regulation of the YAP pathway at P8. (*A* and *B*) Sox9 (green) and α-SMA (red) immunostaining. α-SMA staining was observed in smooth muscle cells in vessel walls in (*A*) controls, whereas SMA was activated ectopically in periductal cells in (*B*) mutants. (*C* and *D*) YAP (red) and Sox9 (green) immunostaining. (*E* and *F*) YAP (red) and amylase (green) immunostaining. (*D* and *F*) Nuclear YAP immunostaining is localized ectopically in periductal and acinar cells in mutants. (*G*) RT-qPCR analysis of YAP transcriptional targets. (*H–M*) YAP (red) and Sox9 (green) immunostaining. Merged images show YAP/Sox9 colocalization in ductal cells in (*J'*) controls and (*M'*) mutants. (*N–S*) YAP (red) and amylase (green) immunostaining. No YAP/amylase colocalization is present in (*P'*) controls, whereas amylase+ cells show YAP+ nuclear staining in (*S'*) mutants. Nuclei were stained with 4′,6-diamidino-2-phenylindole (DAPI) (blue). *Scale bars*: (*A–F*) 50 μm; (*H–S*) 20 μm. $^{**}P < .01$. Control, n = 7; mutant, n = 7 for RT-qPCR and control, n $\geq$ 3; mutant, n $\geq$ 3 for immunostainings.

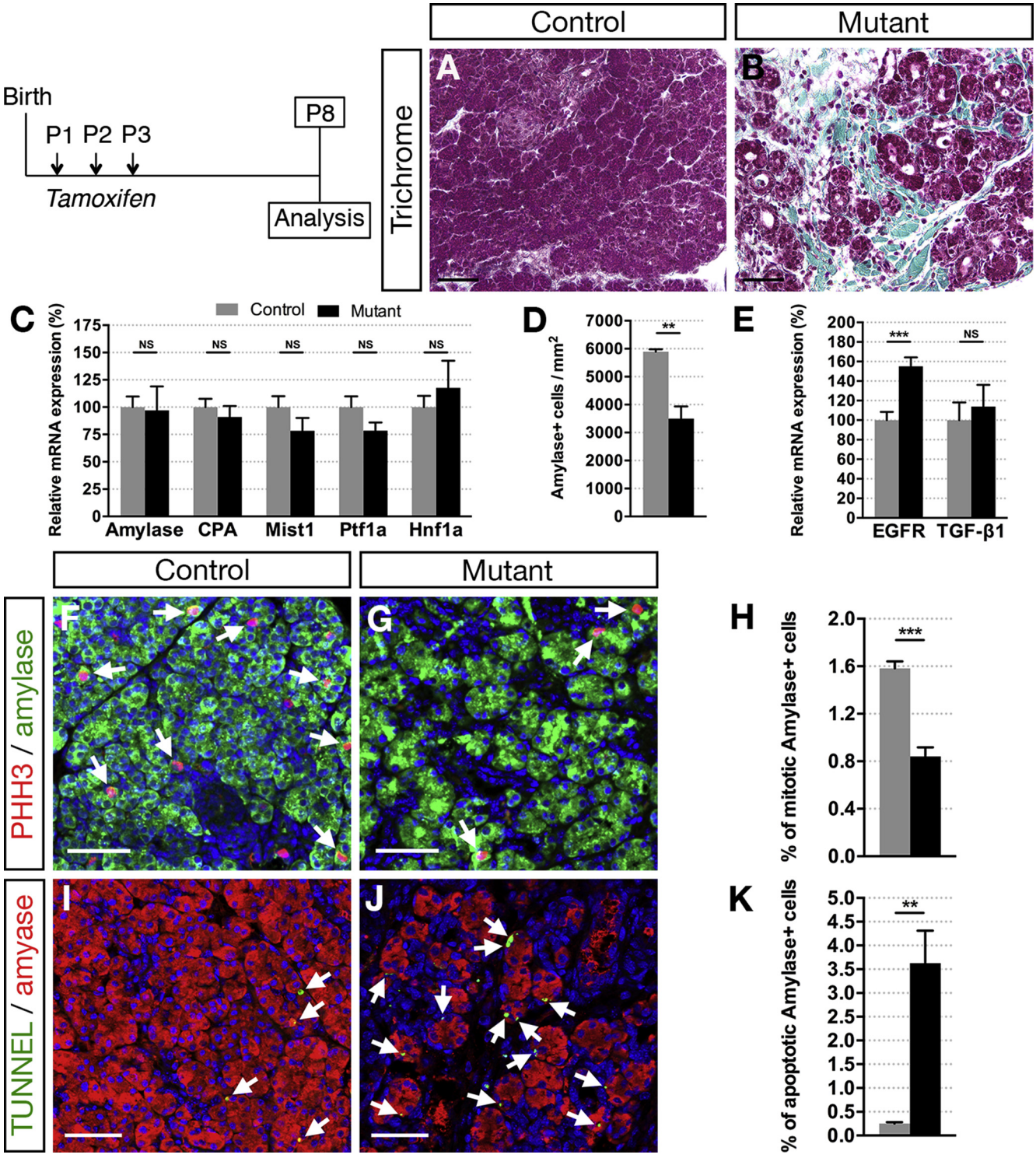

Figure 3. Ductal deletion of *Hnf1b* induces pancreatic fibrosis and loss of acinar cells by P8. (*A* and *B*) Masson's trichrome staining shows collagen deposition in green in mutants. (*C*) RT-qPCR analysis of acinar markers. (*D*) Number of amylase$^+$ cells per area. (E) RT-qPCR of *EGFR* and *TGF-β1*. (*F* and *G*) Phosphohistone H3 (PHH3, red) and amylase (green) immunostaining. *Arrows* indicate mitotic amylase$^+$ cells. (*H*) Quantification of acinar cell proliferation (amylase+ PHH3+/ amylase+ cells). (*I* and *J*) TUNEL assay (green) and amylase (red) immunostaining. *Arrows* indicate apoptotic amylase$^+$ cells. Nuclei are stained with 4′,6-diamidino-2-phenylindole (blue). (*K*) Quantification of acinar cell apoptosis. *Scale bars*: 50 μm. Control, n = 4; mutant, n = 4 for quantification of immunostainings, and control, n = 7; mutant, n = 7 for RT-qPCR. $^{**}P < .01$; $^{***}P < .001$.

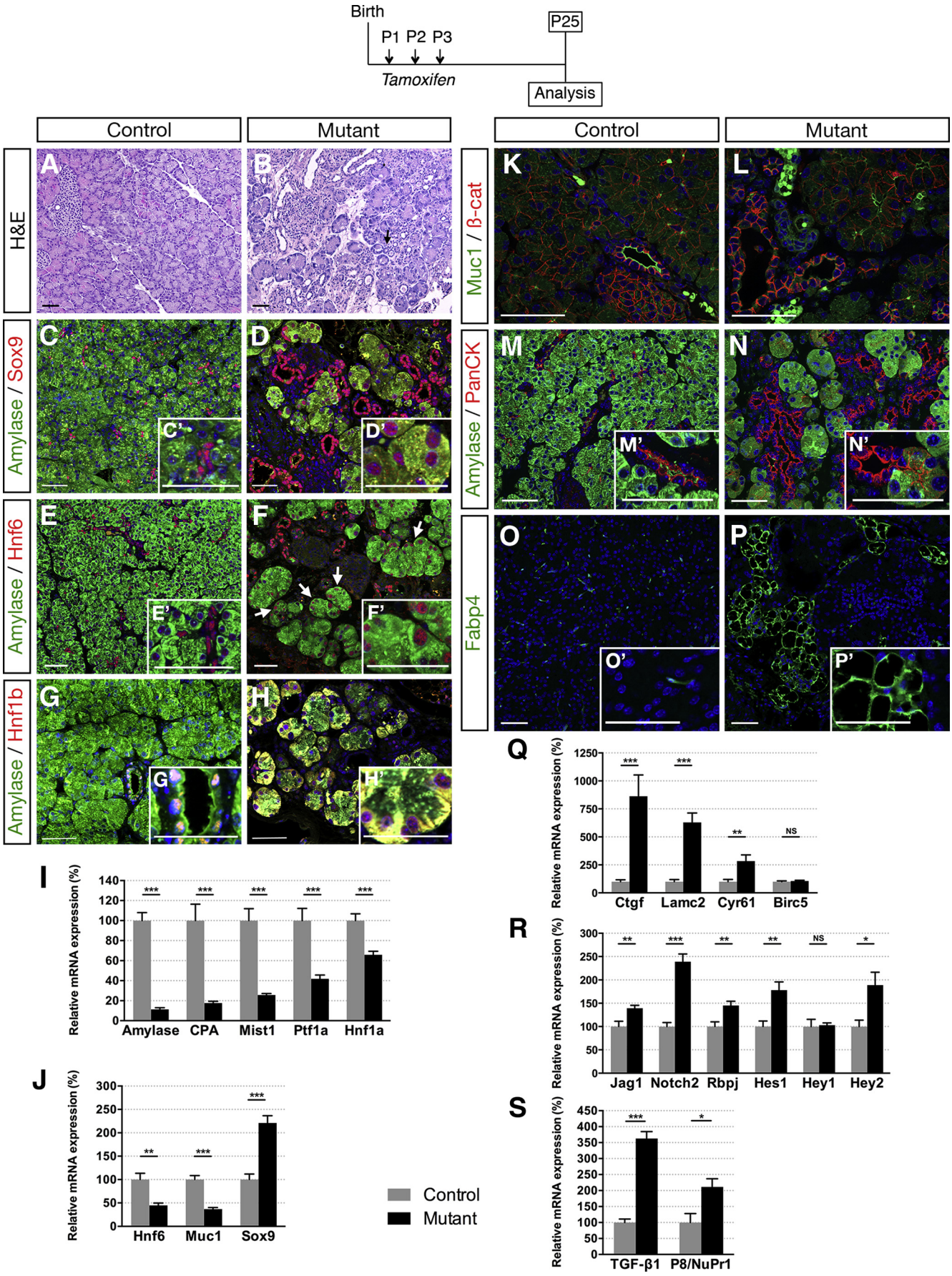
Birth
P1 P2 P3
Tamoxifen
P25
Analysis
Control
Mutant
H&E
Amylase / Sox9
Amylase / Hnf6
Amylase / Hnf1b
Muc1 / β-cat
Amylase / PanCK
Fabp4
Relative mRNA expression (%)
Amylase CPA Mist1 Ptf1a Hnf1a
Hnf6 Muc1 Sox9
Control
Mutant
Ctgf Lamc2 Cyr61 Birc5
Jag1 Notch2 Rbpj Hes1 Hey1 Hey2
TGF-β1 P8/NuPr1

involvement in extracellular matrix fibrosis.[28,29] Accordingly, we observed a marked increase in periductal collagen deposition as indicated by histologic analysis with Masson's trichrome at P8 (Figure 3*A* and *B*, green areas). These changes are reminiscent of pancreas fibrosis, which often is associated with ADM. Because it was recently shown that YAP activity is necessary and sufficient for ADM and pancreatitis induction,[30–32] we examined whether acinar cells were secondarily affected in mutants. Although we found no significant changes in acinar gene expression by RT-qPCR at P8 (Figure 3*C*), at this stage we already observed a 41% decrease in the number of amylase+ cells (Figure 3*D*). We found an up-regulation of *EGFR* expression in mutants (1.6-fold), whereas *TGFβ-1* remained unchanged at this stage (Figure 3*E*), both known to promote ADM.[33–35] Moreover, amylase/PPH3 immunostaining quantifications showed a 47% decrease in acinar cell proliferation (Figure 3*F*–*H*), whereas terminal deoxynucleotidyl transferase–mediated deoxyuridine triphosphate nick-end labeling (TUNEL) assay showed a 15.5-fold increase in acinar cell apoptosis (Figure 3*I*–*K*) in mutants compared with controls. Hence, a combined reduction in acinar cell proliferation and an increase in apoptosis leads to acinar cell loss. Then, large areas of ADM were observed at P25 in mutants (Figure 4*A* and *B*), associated with a dramatic decrease in acinar gene expression (89% for amylase) (Figure 4*I*) and a strong up-regulation of Sox9 (2.2-fold) (Figure 4*J*). Moreover, Sox9 and Hnf6 were expressed ectopically in some acinar cells in mutants (Figure 4*E*–*H*), characterizing ADM.[36] As previously shown in a model of transforming growth factor (TGF)-β–induced ADM,[37] we also found ectopically induced Hnf1b expression in acinar cells at P25 (Figure 4*C* and *D*). At this stage, ducts were more affected than at P8, as indicated by the complete loss of Muc1 apical staining in mutants (Figure 4*K* and *L*), which corroborated with the dramatic decrease in *Muc1* transcript levels (Figure 4*J*). We found a 55% decrease in *Hnf6* expression (Figure 4*J*), with few Hnf6+ cells remaining in mutant ducts compared with ductal Sox9+ cells (Figure 4*C*–*F*), in agreement with our finding that *Hnf6* is a direct target of Hnf1b during pancreas development.[13] By amylase/Pan-cytokeratin co-immunostainings, acinar structures appear closely connected with this ductal network and, more importantly, Pan-cytokeratin co-localized with some amylase+ cells in mutants (Figure 4*M* and *N*). We noticed sparse areas with fat infiltration only in mutants and identified that these fat-containing cells were adipocytes using the Fabp4 marker (Figure 4*O* and *P*), fatty replacement of pancreatic parenchyma often is associated with pancreatic fibrosis and pancreatitis.[4] The YAP pathway was up-regulated dramatically in mutants, stronger than at P8: 8.6-fold for *Ctgf*, 6.3-fold for *Lamc2*, and 2.8-fold for *Cyr61* (Figure 4*Q*). The Notch pathway was shown to be activated during acinar dedifferentiation and to promote ADM.[38] We found up-regulation of most of the Notch components (Figure 4*R*), and especially a 2.4-fold increase in *Notch2* expression, a receptor confined to ducts by embryonic day (E)15.5.[39] Moreover, we observed a significant increase in *Jag1* expression, which was shown to be up-regulated in expanded ducts of chronic pancreatitis patients.[40] At this stage, we also observed a strong increase (3.6-fold) in *TGF-β1* expression in mutants and a significant increase in *p8/Nupr1* expression (Figure 4*S*), a transcriptional co-factor expressed only at low levels in normal pancreata but induced in the initial phases of pancreatitis.[41]

Hence, *Hnf1b* loss of function in ducts leads to loss of acinar cells and ADM, as well as lipomatosis in the pancreas, together with the up-regulation of Yap, Notch, and TGF-β1 pathways.

Postnatal Inactivation of Hnf1b in Ducts Leads to Chronic Pancreatitis in Adults

We further investigated the progression in adults of the pancreatic exocrine disorder associated with ductal *Hnf1b* deficiency. We observed a 43% decrease in pancreas weight at 2 months in mutants, whereas mouse weight was unchanged compared with controls (Figure 5*A*). At 5 months, mouse weight was decreased significantly in mutants as a consequence of pancreatic exocrine deficiency (data not shown). The decreased pancreatic weight was correlated with a dramatic loss of acinar tissue (Figure 5*B* and *C*), correlated with a 95% decrease in acinar gene expression (Figure 5*I*). Many lobes of *Hnf1b*Δ^{duct} mutant pancreata were entirely devoid of acinar tissue and merely consisted of isolated ducts embedded within a large mass of fat. Extensive ADM was shown by very few acini scattered in the tissue and showing an enlarged lumen (Figure 5*E*), duct-like structures (Figure 6*F*), and a strong Sox9 ectopic localization in acinar cells (Figure 5*G* and *H*). Mutant pancreata showed inflammation (Figure 5*J*). We observed a dramatic increase in *F4/80* expression, a marker of macrophages, and in *CD2* expression, a marker of T cells, whereas expression of *CD19*, a marker of B cells, was unchanged (Figure 5*K*). In correlation, we found up-regulation of CCL2, CCL5, and *CXCL10*, showing the involvement of these chemokines in the mutant inflamed pancreas. Infiltration of macrophages also was observed by F4/80 immunostaining (Figure 5*L* and *M*), having an important role in the pathogenesis of

Figure 4. (***See previous page***). **Ductal deletion of *Hnf1b* leads to ADM and lipomatosis at P25.** (*A* and *B*) H&E staining. *Arrows* show acini with increased lumen size in mutants, a feature of ADM. (*C* and *D*) Amylase (green) and Hnf1b (red) immunostaining. (*E* and *F*) Amylase (green) and Sox9 (red) immunostaining. (*G* and *H*) Amylase (green) and Hnf6 (red) immunostaining. *Arrows* show amylase+ cells with nuclear Hnf6+ staining, which is characteristic of ADM in mutants. (*I*) RT-qPCR of acinar markers. (*J*) RT-qPCR of *Hnf6*, *Muc1*, and *Sox9*. (*K* and *L*) Muc1 (green) and β-Cat (red) immunostaining. Muc1 staining is lost at the apical surface of ductal cells in mutants. (*M* and *N*) Amylase (green) and Pan-cytokeratin (red) immunostaining. (*N'*) PanCK localization is expanded in acinar cells of mutants. (*O* and *P*) FABP4 immunostaining shows adipocytes in mutants. (*Q*) RT-qPCR of YAP transcriptional targets (*R*) RT-qPCR of Notch signaling components. (*S*) RT-qPCR of *TGF-β1* and *P8/NuPr1*. *Scale bars*: 50 μm. Nuclei are stained with 4′,6-diamidino-2-phenylindole (blue). Control, n $\geq$ 3; mutant, n $\geq$ 3 for immunostainings; and control, n = 7; mutant, n = 8 for RT-qPCR. *$P < .05$; **$P < .01$; and ***$P < .001$.

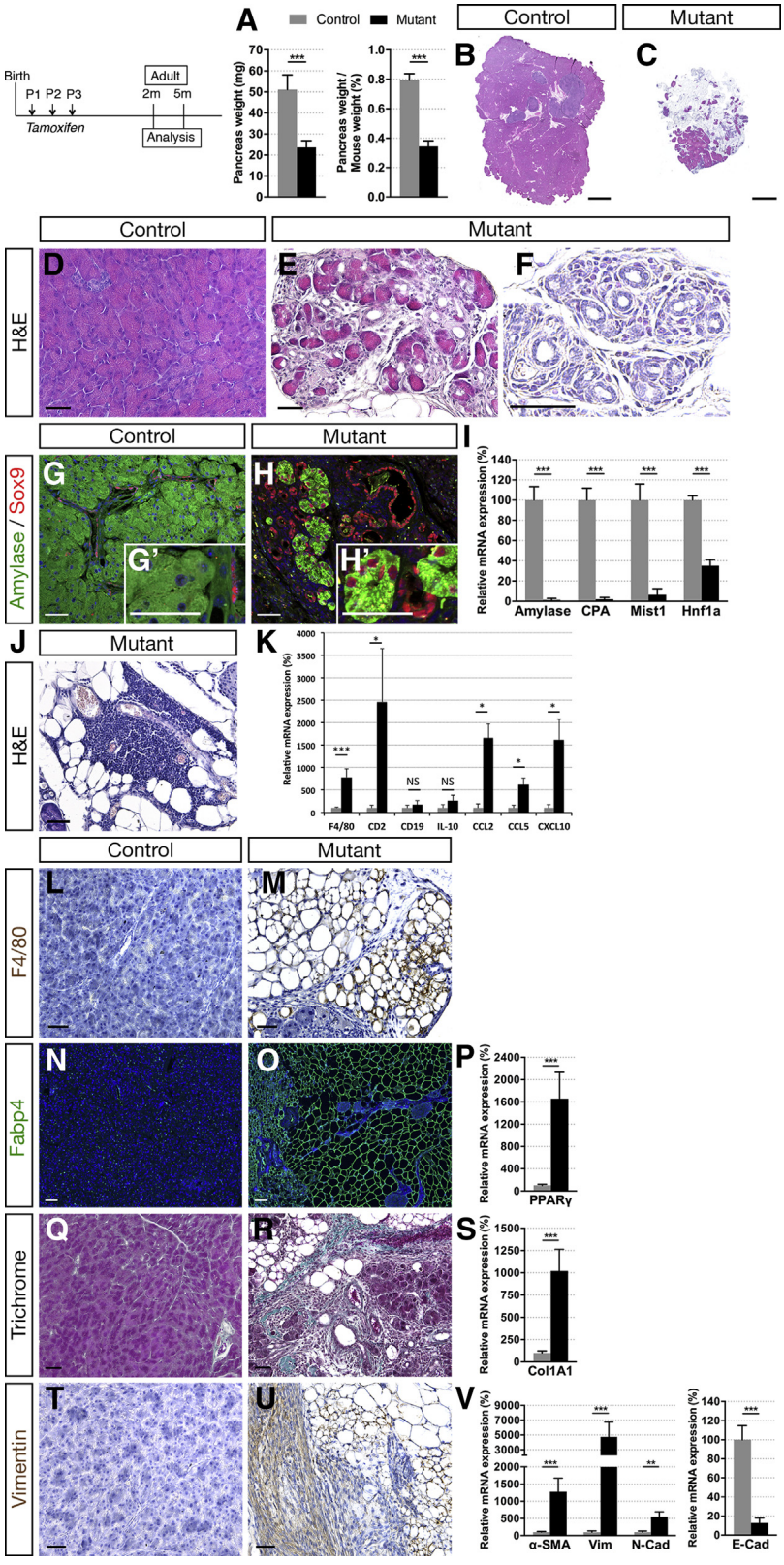

Figure 5. Ductal deletion of *Hnf1b* leads to chronic pancreatitis at 2 months. (*A*) Pancreas weight and relative pancreas weight/body weight of 2-month-old mice (control, n = 17; mutant, n = 11). (*B–F*) H&E staining. Mutant pancreata show dramatic loss of (*C*) acinar tissue and (*E* and *F*) ADM. (*G* and *H*) Amylase (green) and Sox9 (red) immunostaining. (*H'*) Nuclear Sox9+ staining in amylase+ cells is characteristic of ADM in mutants. (*I*) RT-qPCR of acinar markers. (*J*) H&E staining shows lymphocyte infiltration and lipomatosis in mutants. (*K*) RT-qPCR of immune infiltrates (*F4/80*, *CD2*, *CD19*), cytokines (*IL10*), and chemokines (*CCL2, CCL5, CXCL10*). (*L* and *M*) Macrophage marker F4/80 (brown) immunostaining. (*N* and *O*) Adipocyte marker Fabp4 (green) immunostaining and (*P*) RT-qPCR of *PPARγ*. (*Q* and *R*) Masson's trichrome staining. (*S*) RT-qPCR of *Col1A1*. (*T* and *U*) Vimentin (brown) immunostaining. (*V*) RT-qPCR of *SMA*, *vimentin* (Vim), *N-Cad*, and *E-Cad*. *Scale bars*: (*B* and *C*) 2 mm; (*D–H*, *J*, *L*, *M*, and *Q–U*) 50 μm; and (*N* and *O*) 100 μm. Nuclei are stained with 4′,6-diamidino-2-phenylindole (blue). Control, n $\geq$ 3; mutant, n $\geq$ 3 for immunostaining; and control, n = 8; mutant, n = 5 for RT-qPCR. $^{**}P < .01$; $^{***}P < .001$. mRNA, messenger RNA.

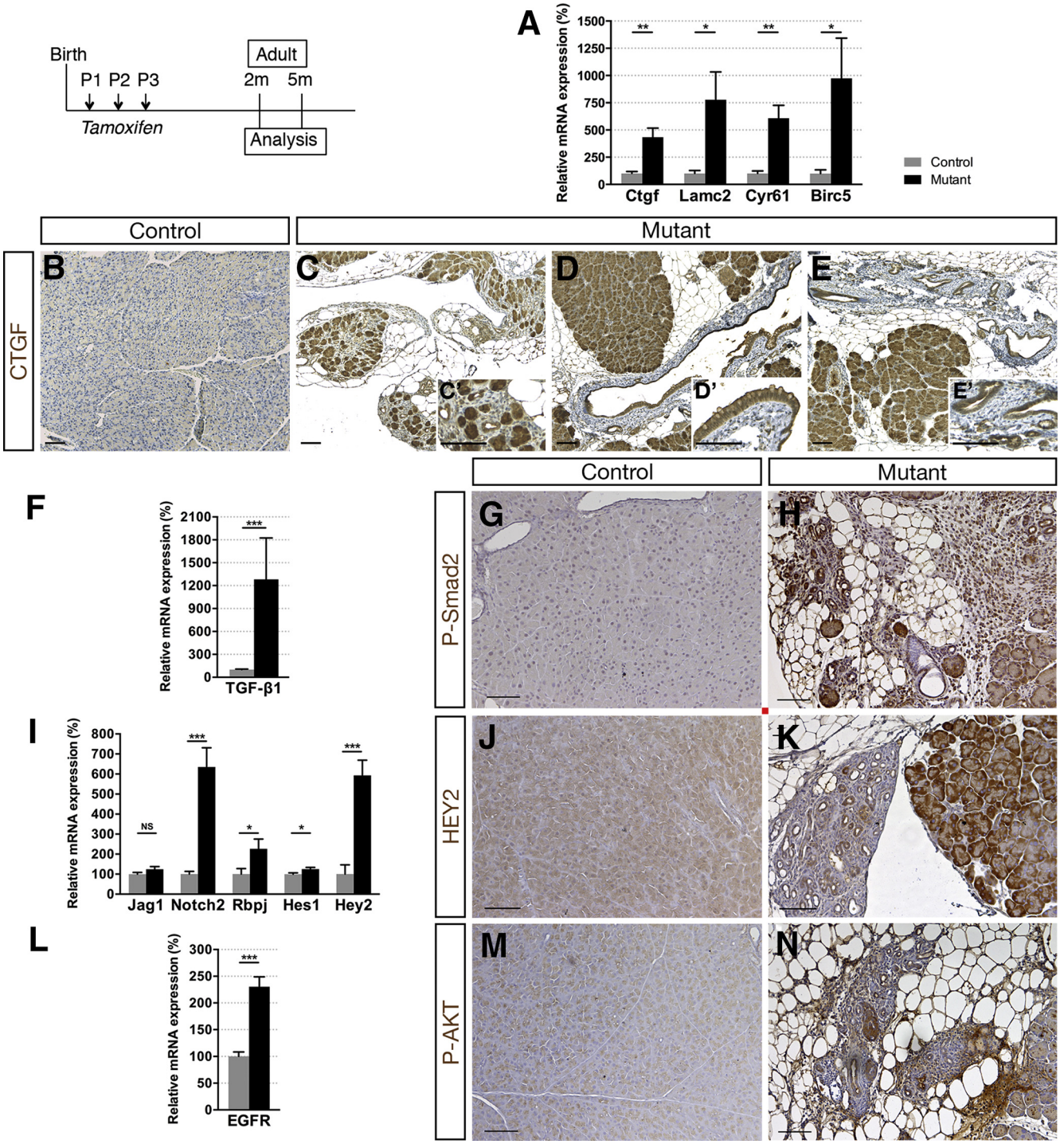

Figure 6. Ductal deletion of *Hnf1b* leads to enhanced signaling pathways that favor tumorigenesis. (*A*) RT-qPCR of YAP transcriptional targets. (*B–E*) CTGF (brown) immunohistochemistry. A strong ectopic CTGF staining was observed in (*C'*) acinar cells in mutants in (*D'*) the epithelium of metaplastic ducts and (*E'*) in PanIN. (*F*) RT-qPCR of the Notch pathway. (*G* and *H*) HEY2 immunohistochemistry. (*I*) RT-qPCR of *TGF-β1*. (*J* and *K*) Phospho-SMAD2 (Ser465, Ser467) immunohistochemistry. (*L*) RT-qPCR of *EGFR*. (*M* and *N*) Phospho-AKT (Ser473) immunohistochemistry. Nuclei were counterstained with hematoxylin. *Scale bars*: 100 μm. Control, n ≥ 3; mutant, n ≥ 3 for immunohistochemistry; and control, n = 6; mutant, n = 5 for RT-qPCR. **P* < .05; ***P* < .01; ****P* < .001.

pancreatitis. Moreover, extensive lipomatosis was observed in mutants (Figure 5*J*). Fabp4 immunostaining showed extended areas of adipocytes (Figure 5*N* and *O*), and *PPARγ* expression, a key player in adipocyte differentiation,[42] was increased dramatically (16.6-fold) in mutants (Figure 6*P*). The pancreatic parenchyma of the mutant was replaced by fibrotic tissue as shown by Masson's trichrome (Figure 5*Q* and *R*) and a 10.2-fold increase in the expression of the

desmoplasia-associated marker *Col1A1* in mutants (Figure 5*S*). We observed a 12.8-fold increase in *α-SMA* expression in mutants, showing pancreatic stellate cell (PSC) activation, a key mediator in the fibrosis observed in the desmoplastic reaction[43] (Figure 5*V*). Interestingly, we found a strong accumulation of the mesenchymal-related protein vimentin in mutants (Figure 5*T* and *U*) correlated with a dramatic increase in *vimentin* expression (47.7-fold) (Figure 5*V*), as well as up-regulation of another mesenchymal marker, *N-cadherin* (5.5-fold). Inversely, the epithelial marker *E-cadherin* was down-regulated dramatically (87%), showing epithelial-mesenchymal transition (EMT).

Thus, inflammation, fibrosis, and activation of PSCs and EMT promote chronic pancreatitis in adult *Hnf1b*Δ^{duct} mutants.

Postnatal Inactivation of Hnf1b in Ducts Leads to Pancreatic Neoplasia and Potentiates Kras^{G12V}-Driven PanIN Formation

Chronic pancreatitis has been shown to predispose to pancreatic cancer.[1] Activated signaling pathways play a role in ADM and also in early PanIN lesions. We therefore investigated the potential development of PanINs in adult *Hnf1b*Δ^{duct} mutants.

Connective tissue growth factor (CTGF) production is abundant in the desmoplastic stroma present in pancreatic cancer.[44] We found a 4.4-fold increase of *Ctgf* expression in adult *Hnf1b*Δ^{duct} mutants (Figure 6*A*), and strong ectopic CTGF protein localization in acinar cells in mutants compared with controls (Figure 6*B* and *C*). Moreover, we observed strong CTGF expression in the epithelium of metaplastic ducts (Figure 6*D*) and in neoplastic lesions (Figure 6*E*) in *Hnf1b*Δ^{duct} mutants. *Cyr61* recently was reported to be expressed in PanINs, Cyr61 signaling being critical for EMT and promoting pancreatic carcinogenesis.[45] We found a dramatic increase (6.1-fold) of *Cyr61* in adult *Hnf1b*Δ^{duct} mutants, as well as *Lamc2* and *Birc5*, other markers of the YAP pathway (Figure 6*A*).

TGF-*β* pathway activation plays a crucial role in pancreatic tumor initiation through its capacity to induce ADM, providing a favorable environment for neoplasia.[37] We found a 12.8-fold increase in *TGF-β1* expression in mutants compared with controls (Figure 6*F*), with a 4-fold increase compared with mutants at P25. Moreover, phospho-Smad2 protein was strongly localized ectopically in the nuclei of ADM structures, metaplastic ducts, and fibrotic tissue (Figure 6*G* and *H*), monitoring the activation of the TGF-*β* signaling pathway in adult *Hnf1b*Δ^{duct} mutants.

Ectopic Notch activation, promoting both initiation and progression of PanINs, is also an early event in pancreatic carcinogenesis.[46] We found a strong up-regulation of Notch pathway components, higher than at P25, especially for the receptor *Notch2* and the effector *Hey2* (6.4-fold and 5.9-fold, respectively) (Figure 6*I*). In correlation, Hey2 protein was observed ectopically in acinar cells, in enlarged ducts, and in ADM structures in mutants (Figure 6*J* and *K*). Aberrant activation of epidermal growth factor receptor (EGFR) signaling is also essential in pancreatic tumorigenesis[34] and we observed a strong up-regulation of *EGFR* (2.3-fold) (Figure 6*L*) in adult *Hnf1b*Δ^{duct} mutants, along with a strong localization of phospho-AKT in the fibrotic and inflamed tissue of the mutant pancreas (Figure 6*M* and *N*).

Remarkably, histologic analysis showed intraepithelial neoplasia as low-grade PanINs in *Hnf1b*Δ^{duct} mutant pancreata (Figure 7*A*). These were characterized by an epithelium composed of tall columnar cells with basally located nuclei with light atypia, a pseudostratified architecture and abundant supranuclear mucin. These neoplastic structures were Alcian blue–positive (Figure 7*B*) and positive for the PanIN-specific marker claudin 18 (Figure 7*C*). Thus, loss of *Hnf1b* leads to pancreatic neoplasia by 2 months. By GFP immunostainings, we performed a lineage tracing analysis and found no GFP signal in ADM/PanIN in Hnf1b mutants, strongly suggesting that PanIN-like structures derived indirectly from Hnf1b-ablated YFP+ ductal cells, by a non–cell autonomous mechanism (Figure 7*D*).

By quantification of the acinar compartment in mutants, 11.6% of remaining acini, 80.8% of adipocytes, 6.1% of fibrosis/infiltrates, 1.3% of ADM, and 0.5% of PanIN were observed in mutants (Figure 7*E*). By analyzing older animals until 18 months, we did not observe PanIN progression (data not shown). We then investigated if loss of Hnf1b could promote tumorigenesis in the context of oncogenic Kras (Kras^{G12V}). Somatic activating mutations in Kras indeed appear in 97% of PDAC patients, but additional factors are required to initiate PanIN progression and PDAC. To activate Kras in acinar cells, we used the Elas-tTA; TetO-Flpase; FRT-Stop-FRT Kras^{G12V} mouse line. Untreated mice (without doxycycline) develop PanIN lesions with long latency, with low-grade PanIN from 5 to 6 months. We crossed these mice, hereafter referred to as *Kras*, with Sox9-CreER;Hnf1b$^{fl/fl}$ mutants to obtain Elas-tTA; TetO-Flpase; FRT-Stop-FRT Kras^{G12V}/Sox9-CreER;Hnf1b $^{fl/fl}$ with TM induction perinatally, hereafter referred to as *Kras;mutants*. Histologic analyses by H&E staining (Figure 8*A*), Alcian blue staining (Figure 8*B*), and claudin 18 immunohistochemistry (Figure 8*C*) at 5 months showed large area of PanINs in Kras;mutants compared with mutants and age-matched Kras, affecting more lobules with a very large amount of lesions. This showed that a combination of Hnf1b deletion with oncogenic KRAS activation enhanced pancreatic damage at 5 months relative to oncogenic KRAS alone. Quantification of Alcian blue–positive lesions showed a dramatic increase in the surface of lesions in mutant;Kras compared with mutants and Kras (Figure 8*D*), which was the result of a combined increase in the number of lesions (Figure 8*E*) and in the size of the lesions (Figure 8*F*) in mutant;Kras. Moreover, we observed increased progression of PanIN lesions up to high grade at 5 months in mutant;Kras (Figure 8*G*–*K*). Thus, Hnf1b inactivation in ducts provides a propitious environment for the onset of KRAS^{G12D}-induced PanINs.

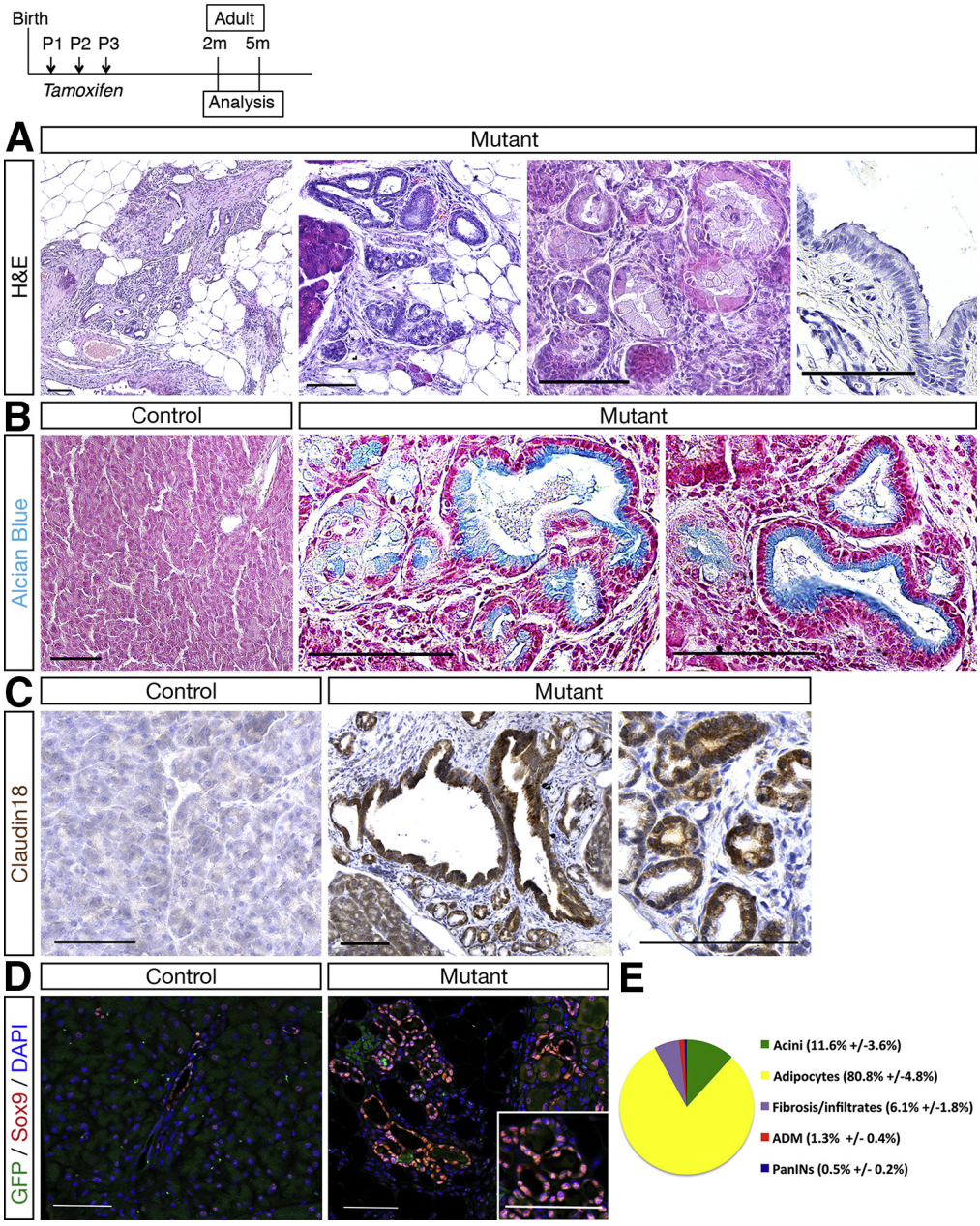

Figure 7. Ductal deletion of *Hnf1b* leads to PanIN by 2 months. (*A*) H&E staining of mutant pancreata showing epithelial structures composed of columnar cells with abundant supranuclear cytoplasm and basally located nuclei. (*B*) Alcian blue staining. Columnar mutant epithelial cells showed blue-stained supranuclear mucin. (*C*) PanIN marker claudin 18 (brown) immunohistochemistry. (*D*) Sox9 (red) and GFP (green) immunostaining. Sox9+ ADM structures did not derive from Hnf1b-targeted GFP+ cells. (*E*) Quantification of the relative surface of acini, adipocytes, fibrosis/infiltrates, ADM, and PanINs in mutants (n = 6). *Scale bars*: 100 μm. Control, n $\geq$ 3; mutant, n $\geq$ 3 for histology and immunohistochemistry. DAPI, 4′,6-diamidino-2-phenylindole.

Adult Inactivation of Hnf1b in Ducts Leads to Impaired Acinar Regeneration After Cerulein-Induced Pancreatitis

We next tested the hypothesis that *Hnf1b* could be required for maintenance of exocrine homeostasis in the adult. We inactivated *Hnf1b* in adult ductal cells, with TM injections on 6-week-old mice, and observed the consequences on the pancreatic tissue at 9 weeks and 20 weeks. We did not observe changes in the pancreatic weight in these mutants compared with controls (Figure 9*A* and *C*). Analysis of acinar marker expression by RT-qPCR (Figure 9*B* and *D*) and H&E staining (Figure 9*E* and *F*) yielded no overt pancreatic pathology at either time point when *Hnf1b* was inactivated in adult ducts, probably owing to the lower proliferation rate of adult ductal cells compared with postnatal ductal cells.[5] Thus, we investigated if loss of *Hnf1b* in adults would sensitize acinar cells to injury-induced reprogramming because ductal cells are capable of contributing to acinar regeneration.[47,48] Two weeks after TM in adults, acute pancreatitis was induced by 2 consecutive days of treatment with the secretagogue cerulein, and pancreata were harvested 1 week later (Day [D]7). We verified that *Hnf1b* inactivation also was efficient at this stage, and observed a 50% decrease in *Hnf1b* expression in $Hnf1b\Delta^{\text{adult duct}}$ mutants (Figure 10*A*). We followed *amylase* expression by RT-qPCR and found no significant changes between controls and mutants at D0 and D3. *Amylase* expression was

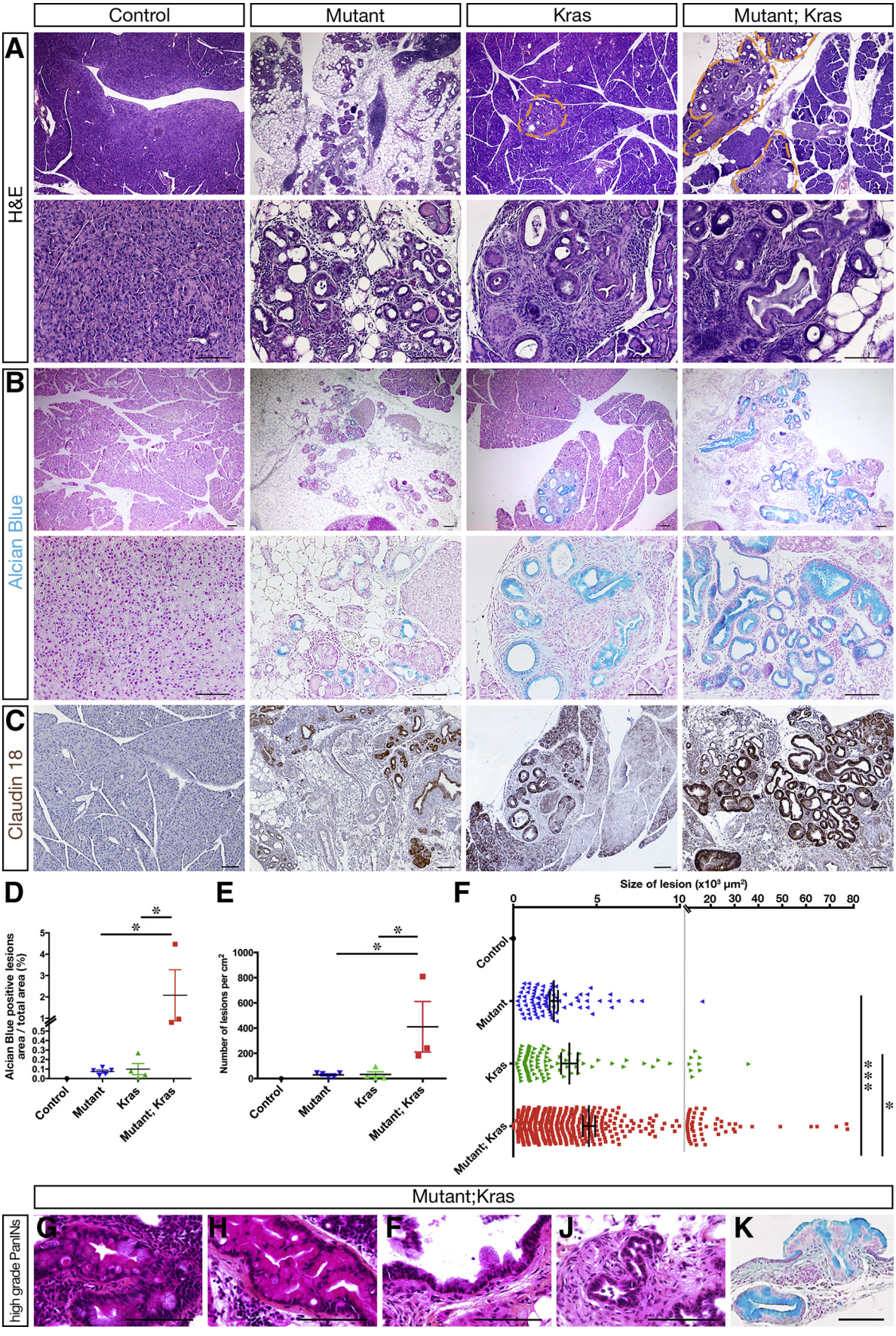
Control
Mutant
Kras
Mutant; Kras
A
H&E
B
Alcian Blue
C
Claudin 18
D
Alcian Blue positive lesions area / total area (%)
Control
Mutant
Kras
Mutant; Kras
E
Number of lesions per cm²
F
Size of lesion (x10³ µm²)
0
5
10
20
30
40
50
60
70
80
Control
Mutant
Kras
Mutant; Kras
***
*
Mutant;Kras
high grade PanINs
G
H
F
J
K

decreased dramatically at D3, showing the efficiency of cerulein treatment (Figure 10*B*). Although controls showed a recovery of *amylase* expression at D7, *Hnf1b*Δ$^{adult\ duct}$ mutants were unable to recover after injury, showing dramatically low levels of *amylase* expression in mutants (99% decrease). Other acinar markers showed the same pattern of expression with critically low levels of *CPA*, *Ptf1a*, *Mist1*, and *Nr5a2* expression in *Hnf1b*Δ$^{adult\ duct}$ mutants compared with controls at D7 (Figure 10*C*). In mutants, we observed a dramatic increase in *F4/80* and *CD2* expression, whereas expression of the B-cell marker *CD19* was unchanged (Figure 10*D*), showing increased severity of pancreatitis in mutants with macrophages and T-cell recruitment. We found a tendency but not a significant increase in the messenger RNA level of *CCL2, CCL5*, and *CXCL10* chemokines in mutants at D7, suggesting that the chronic pancreatitis was more established in *Hnf1b* mutants at 5 months after perinatal inactivation (Figure 5*K*) than in adult *Hnf1b* mutants 7 days after cerulein treatment (Figure 10*D*). Histologic analysis by H&E and Masson's trichrome staining showed no abnormalities at D0, but ADM and interstitial fibrosis at D3 both in controls and mutants. At D7, although control pancreata were recovered, we observed persistent and strong defects in *Hnf1b*Δ$^{adult\ duct}$ mutant pancreata, characteristic of chronic pancreatitis (Figure 10*E*). No large amylase+ acinar clusters were detected in *Hnf1b*Δ$^{adult\ duct}$ mutant pancreata in contrast to controls, and co-localization of Sox9 and amylase was observed in almost all acinar cells in *Hnf1b*Δ$^{adult\ duct}$ mutant pancreata (Figure 10*F* and *G*), showing widespread ADM at D7. Remarkably, we observed abundant persistent metaplastic lesions, fibrosis, and formation of neoplastic lesions, as shown by histology on H&E (Figure 10*H* and *I*), Alcian blue staining (Figure 10*J* and K), and by immunohistochemistry with the PanIN-specific marker claudin 18 (Figure 10*L* and *M*). These results show the requirement of Hnf1b in adult ducts for acinar cell regeneration in the context of tissue injury. Our data further suggest that *Hnf1b* deficiency in adult ductal cells in the context of tissue injury can initiate neoplastic lesions.

Discussion

We show that *Hnf1b* inactivation in ductal cells after birth causes loss of primary cilia, duct proliferation, and dilatation. This triggers fibrosis, ADM, inflammatory infiltration, lipomatosis, and activation of PSC and EMT, leading to chronic pancreatitis and PanINs.

Hnf1b *Inactivation in Differentiated Postnatal Pancreatic Ducts Leads to Chronic Pancreatitis*

Ductal *Hnf1b* inactivation leads to a dramatic decrease in cystic disease–associated gene expression, especially *Pkhd1* and *Cys1*, reinforcing our previous findings that they were direct targets of Hnf1b in pancreatic progenitors at E12.5.[13] *Pkhd1*, *Cys1*, and *Tg737/Ift88* play a role in the structural integrity of cilia. The *Pkhd1* gene encodes fibrocystin, a membrane protein localized to the primary cilium of tubular epithelial cells,[49] and a lack of fibrocystin disrupted ciliogenesis in *Pkhd1*-deficient mice.[50] Interestingly, it recently was reported that novel mutations of *PKHD1* are associated with chronic pancreatitis.[51] The *Cys1* gene product, cystin, also localizes to the primary cilium and stabilizes microtubule assembly.[52] The protein IFT88/polaris is a core component of the intraflagellar transport machinery and is required for the formation of cilia.[53] Primary cilia transduce signals from extracellular stimuli to a cellular response that regulates proliferation, differentiation, transcription, migration, polarity, and tissue morphology.[54] They can play a negative role in epithelial cell proliferation.[55] Mutations affecting cilia development promote a dilated ductal phenotype or cyst formation.[8,9,56] In correlation with the loss of primary cilia, we found increased proliferation of ductal cells in *Hnf1b*Δ^{duct} mutant pancreata. Moreover, this leads to duct dilatation and partial loss of apicobasal polarity of epithelial ductal cells. Some *Hnf1b*Δ^{duct} mutant ducts were devoid of primary cilia, although they were not dilated, strongly suggesting that duct dilatation occurs secondary to the loss of primary cilia. Furthermore, Muc1 immunostaining still was observed in some dilated ducts. We observed weaker expression of Muc1 at P25, whereas it was unchanged at P8. This strongly suggests that loss of apicobasal polarity is a consequence of duct dilatation. *Pkhd1* also is involved in the tubulogenesis and/or maintenance of duct-lumen architecture,[49] and its decreased expression likely contributes to duct dilatation in *Hnf1b*Δ^{duct} mutants. Prox1 was down-regulated significantly in *Hnf1b*Δ^{duct} mutants by P8 and it was shown previously that *Prox1* inactivation results in dilated pancreatic ducts and ADM. *Prox1* mutant adult pancreata uncovered features of chronic tissue damage: acinar apoptosis, macrophage infiltration, mild fibrosis, and extensive lipomatosis,[21] suggesting that reduced *Prox1* expression contributes to the phenotype observed in *Hnf1b*Δ^{duct} mutants. Lineage tracing analysis showed that adipocytes of *Prox1* mutant pancreata did not originate from transdifferentiated pancreatic acinar cells,[21]

Figure 8. (*See previous page*). Ductal deletion of *Hnf1b* promotes PanIN progression in a Kras-activated context. Sox9-Cre^{ER};Hnf1b$^{fl/fl}$ mutants were crossed with Elas-tTA; TetO-Flpase; Kras^{G12V} mice (referred to as *Kras*) to obtain Sox9-Cre^{ER};Hnf1b$^{fl/fl}$;Elas-tTA; TetO-Flpase; Kras^{G12V} (referred to as *mutant;Kras*) that combined perinatal inactivation of Hnf1b in ducts and oncogenic activation of Kras^{G12V} in acinar cells. Analyses of the pancreata were performed at 5 months. (*A*) H&E staining. (*B*) Alcian blue staining. (*C*) Claudin 18 (brown) immunostaining. (*D*) Quantification of the surface of the lesions stained with Alcian blue. (*E*) Quantification of the number of lesions per cm^2. (*F*) Quantification of the size of the lesions. (*G–K*) High-grade PanINs in mutant;Kras by (*G–J*) H&E staining and (*K*) Alcian Blue staining. Some lesions present marked cytologic and architectural atypia with the formation of branching papillae. Nuclei are enlarged and hyperchromatic with focal nuclear stratification. *Scale bars*: 100 μm. Mutants, n = 5; Kras, n = 4; mutant;Kras, n = 3. *$P < .05$; ***$P < .001$.

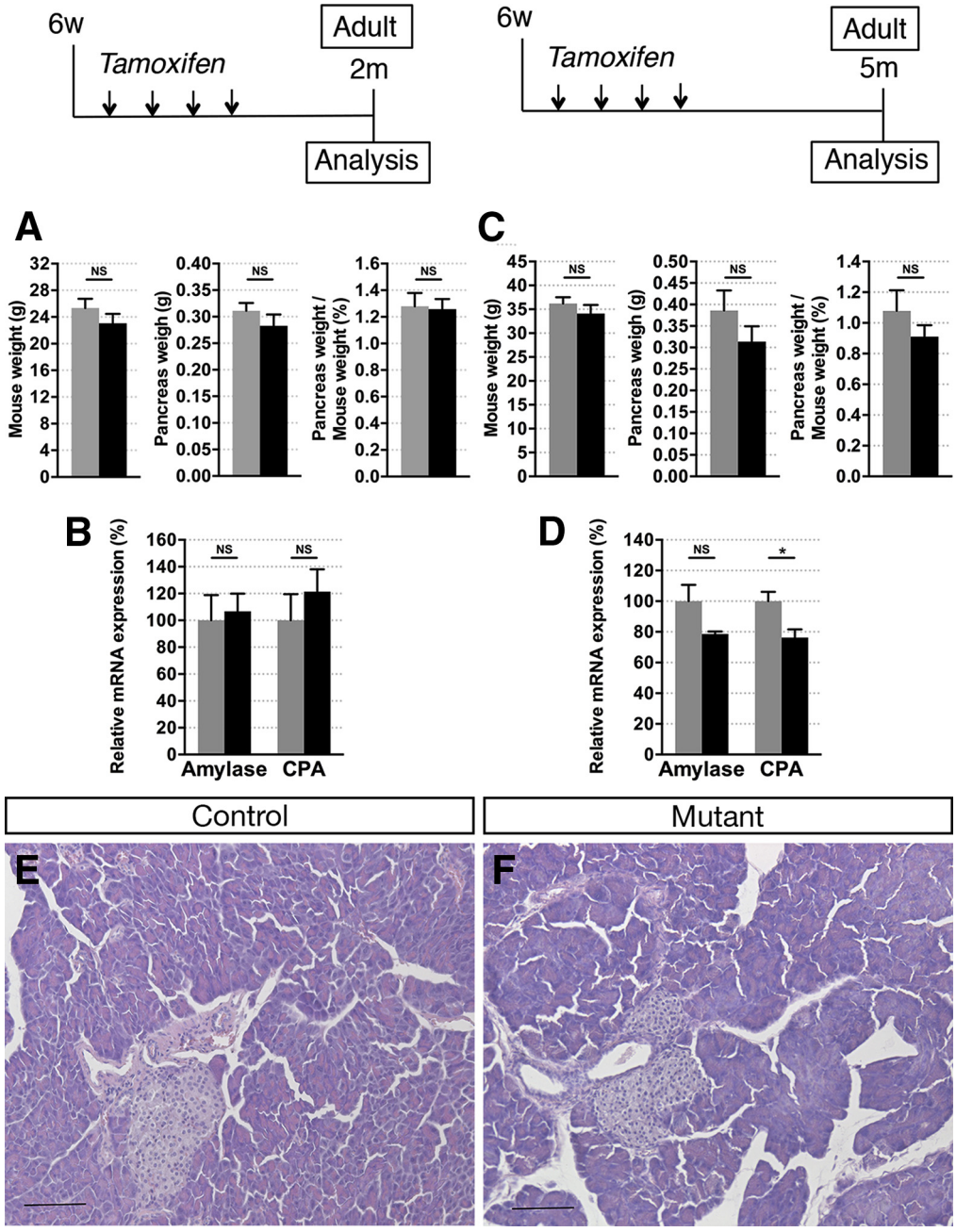

Figure 9. Adult *Hnf1b* inactivation in ductal cells does not lead to obvious perturbation of acinar homeostasis. (*A–F*) Tamoxifen was injected in 6-week-old adult mice and analyses were performed at (*A* and *B*) 2 months or (*C–F*) 5 months. (*A*) Mouse weight, pancreas weight, and relative pancreas weight/body weight of 2-month-old mice. (*B*) RT-qPCR of acinar markers at 2 months. (*C*) Mouse weight, pancreas weight, and relative pancreas weight/body weight of 5-month-old mice. (*D*) RT-qPCR of acinar markers at 5 months. (*E* and *F*) H&E staining of the pancreata at 5 months. *Scale bars*: 100 μm. Control, n $\geq$ 5; mutants, n $\geq$ 5. *$P < .05$. CPA, Carboxypeptidase A.

suggesting that this also may be the case for *Hnf1b*Δ^{duct} mutants, and rather caused by fibroblast activation.[4] Dilated ducts also were reported in pancreata devoid of Hnf6.[56,57] Pancreatitis was observed in *Hnf6* mutant animals,[57] associated with the finding of shorter primary cilia of ductal cells.[58] We observed a decreased expression of *Hnf6* at P25, whereas it was unchanged at P8, showing that loss of Hnf6 can contribute secondarily to the phenotype. Our data further underscore the link between primary cilia and pancreatitis. Defects in cilia have been associated with a spectrum of human diseases collectively called *ciliopathies*.[59] Ductal cysts, polarization defects, dysplasia, and fibrosis of the pancreas have been described in many ciliopathies. The absence of pancreatic cilia during mouse embryogenesis in *Kif3a* mutants or in hypomorphic Tg737 mutants (*Tg737*^{orpk}) resulted in lesions that resemble those found in patients with pancreatitis or cystic fibrosis.[7–9] However, the function of ducts and primary cilia in postnatal pancreatic tissue homeostasis was largely unknown. We show here that *Hnf1b* inactivation leads to loss of primary cilia and duct dilatation, Hnf1b being necessary for the expression of *Pkhd1*, *Cys1*, and *Prox1* in pancreatic ducts. Our results are also of particular interest because genes we found down-regulated in *Hnf1b*Δ^{duct} mutant pancreata also are linked to pancreatic neoplasia.[60–62]

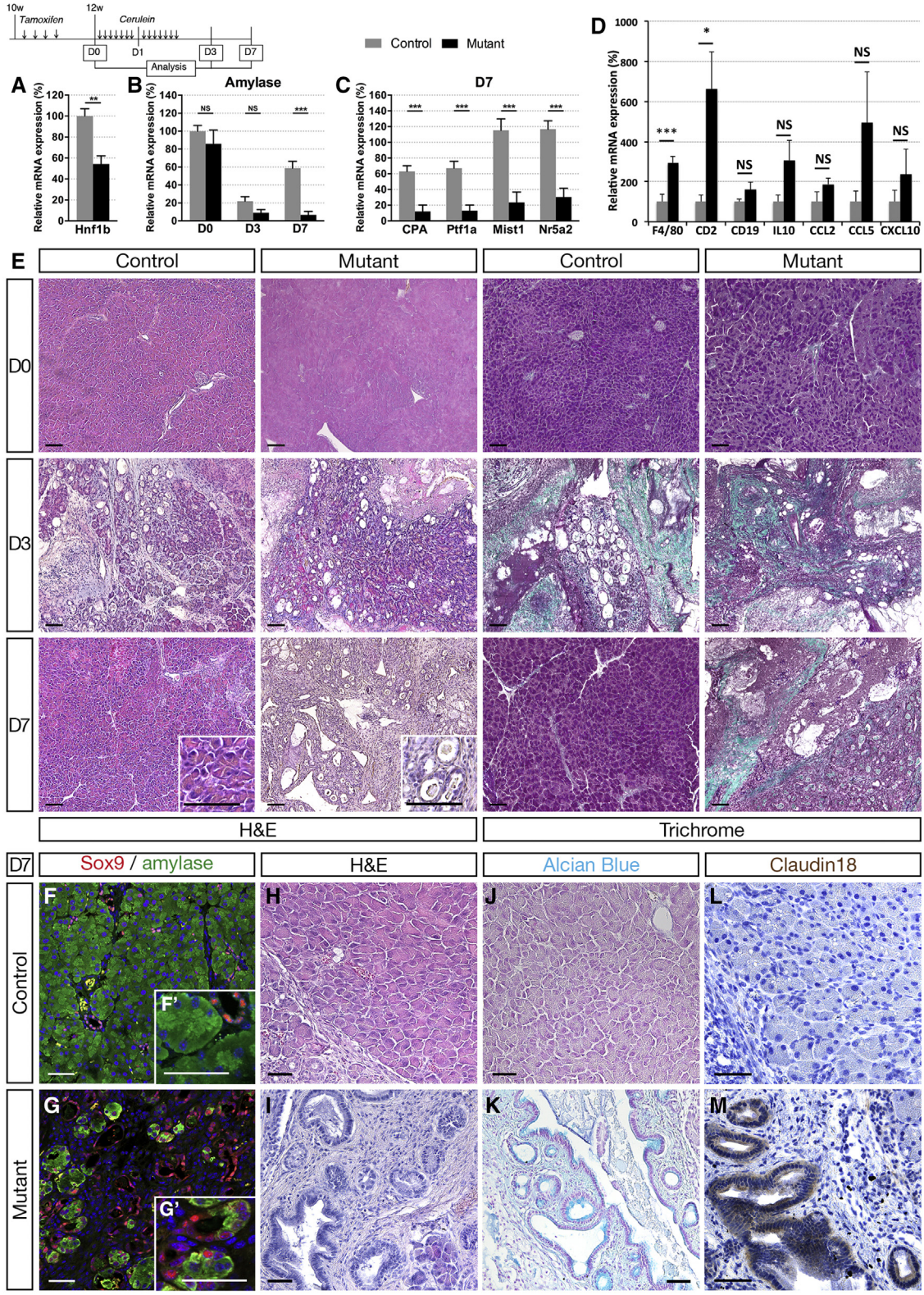

Figure 10. Adult Hnf1b inactivation in ductal cells leads to impaired acinar regeneration and neoplasia after cerulein-induced pancreatitis. (*A*) Analysis of *Hnf1b* inactivation efficiency by RT-qPCR. (*B*) RT-qPCR of *amylase* at D0, D3, and D7. (*C*) RT-qPCR of acinar markers at D7. (*D*) RT-qPCR of inflammatory markers at D7. (*E*) H&E and Masson trichrome staining. (*F* and *G*) Amylase (green) and Sox9 (red) immunostaining showing widespread ADM at D7 in mutants. (*H* and *I*) H&E staining, (*J* and *K*) Alcian blue staining, and (*L* and *M*) claudin 18 (brown) immunostaining showing PanIN in mutants. *Scale bars*: (*E*) 50 μm; (*F–M*) 100 μm. Control, n $\geq$ 5; mutants, n $\geq$ 5 for RT-qPCR; and control, n $\geq$ 3; mutants, n $\geq$ 3 for histology and immunostainings. **P* < .05; ***P* < .01; ****P* < .001.

Hnf1b *Inactivation in Pancreatic Ducts Leads to Neoplasia and Enhances the Ability of Oncogenic KRAS to Promote Precancerous Lesions*

Because cilia have the ability to physically influence the cell cycle and fine-tune signaling cascades, loss of primary cilia may promote tumorigenesis through aberrant signal transduction. Ciliogenesis indeed was found suppressed in tumor cells, including PanINs and PDAC.[63] YAP was shown to promote cell proliferation[64] and we observed an up-regulation of the YAP pathway and an increased proliferation of ductal cells in *Hnf1b*Δ^{duct} mutants. Recent studies have highlighted the role of YAP in the regulation of cell proliferation during postnatal liver growth and cancer pathogenesis, increased YAP activation was associated with hepatic cyst epithelium proliferation in autosomal-recessive polycystic kidney disease.[24] Moreover, YAP functions as a mechanoresponsive transcriptional co-activator.[25–27] Our data suggest that mechanical stress induced by enlarging cysts stimulates YAP activation in pericystic and acinar cells. Because YAP activity is necessary and sufficient for ADM and pancreatitis induction,[30–32] YAP constitutes a molecular link between *Hnf1b* deletion in ductal cells and the non–cell-autonomous effects on acinar cells. Moreover, YAP drives fibrosis by activating fibroblasts.[29] YAP transcriptional targets were progressively overexpressed from P8 to the adult stage: *CTGF* and *Lamc2* from P8, *Cyr61* by P25 and *Birc5* in adults. All of them were strongly up-regulated 4- to 10-fold in adults. In correlation, a 4.5-fold increase in *CTGF* expression was observed in human chronic pancreatitis.[65] CTGF is involved in cell adhesion, cell migration, inflammation, pancreatic fibrosis, tumor growth, and metastasis, and it is overexpressed in human pancreatic cancer.[66] Thus, fibrosis likely is caused by increased *CTGF* expression and this fibrotic microenvironment promotes PanINs in *Hnf1b*Δ^{duct} mutant pancreata. Moreover, LAMC2 recently was identified as a new putative pancreatic cancer biomarker.[67] EGFR, promoting ADM and PanINs,[34] also is involved in ADM induction and formation of neoplastic lesions in *Hnf1b*Δ^{duct} mutants because up-regulation of *EGFR* in mutants was observed from P8, with a 2-fold increase in adults. From P25, Notch and TGF-β signaling contribute to ADM, fibrosis, activation of PSCs, and PanIN development in *Hnf1b*Δ^{duct} mutants, with a 2-fold up-regulation at P25 and 6-fold in adults for Notch signaling, a 4-fold up-regulation at P25 and 13-fold in adults for *TGF-β1* in *Hnf1b*Δ^{duct} mutants. The selective dramatic up-regulations of *Notch2* and *Hey2* in *Hnf1b*Δ^{duct} mutants are in accordance with the finding that centroacinar and terminal ductal epithelial cells did not display up-regulation of *Hes1* transcripts, but did show up-regulated expression of *Hey2* consistent with an active Notch pathway.[68] Moreover, *Notch2* is expressed in ductal cells and PanIN lesions and is a central regulator of PanIN progression and malignant transformation.[69] Notch indeed regulates ADM and promotes both initiation and progression of PanINs.[2,38,46] Because TGF-β was shown to trigger ADM in acinar cells,[37] it would be interesting to further test the requirement of TGF-β activation to drive ADM in *Hnf1b*Δ^{duct} mutants with the use of TGF-β inhibitors. TGF-β signaling also is pivotal in driving fibrogenesis, for activation of PSC, and for PanIN formation.[44,70] Thus, activation of the YAP pathway, EGFR pathway, and subsequent up-regulation of the Notch and TGF-β pathways support the non–cell-autonomous effects leading to ADM, PSC activation, fibrosis, and PanINs in *Hnf1b*Δ^{duct} mutants. Furthermore, we observed an increase in both the number and the grade of PanIN lesions in the pancreas of mice combining both perinatal Hnf1b inactivation in ducts and oncogenic Kras activation in mature acinar cells, showing that loss of Hnf1b promotes PanIN formation in a Kras activated context. Thus, the environment resulting from *Hnf1b* inactivation is favorable for Kras^{G12V}-dependent carcinogenesis.

Increased risk for neoplastic conversion also has been linked to perturbations in pathways that control tissue regeneration.[71] We examined the role of Hnf1b in adult ducts in the process of tissue injury and regeneration in the cerulein-induced acute pancreatitis model.[72] Remarkably, our findings show that *Hnf1b* inactivation in adult ductal cells is associated with impaired acinar regeneration and chronic inflammation, allowing ADM and PanIN formation in the context of tissue injury in adults. Whether this role is owing to Hnf1b function in terminal ducts or centroacinar cells will require further investigations.

HNF1B *Role in Etiology and Physiopathology of the Human Diseases Maturity Onset Diabetes of the Young Type 5, Chronic Pancreatitis, and PDAC*

HNF1B heterozygous mutations are notably associated with maturity onset diabetes of the young type 5 diabetes, pancreas exocrine dysfunction (pancreatitis with reduced fecal elastase concentration in 93% of these cases, fecal fat excretion), and pancreas structural anomalies (atrophy, cysts, calcification).[73] Pancreatitis was surprising to observe because *Hnf1b* is not expressed in acinar cells and it was proposed that this defect might be caused by pancreas hypoplasia. The results of the present study show that pancreatitis associated with *Hnf1b* deficiency is caused by pancreatic duct alteration. Moreover, differences observed from one patient to another might be owing to impaired recovery of the pancreas in adults because our results also show that *Hnf1b* deficiency leads to altered acinar regeneration after injury.

Studies have shown that down-regulation of *HNF1B* is associated with cancer risk, including renal, prostate, ovarian, and colorectal cancers, showing that HNF1B is a marker of these cancers and a potential tumor suppressor.[74–78] Pancreatic cancer is poorly characterized at genetic and nongenetic levels. Recent analyses have suggested that reduced HNF1B activity also could be an important step in pancreatic tumorigenesis. Mutations in *HNF1B* have been identified as markers of pancreatic

cancer risk loci through genome-wide association study analyses.[79–81] In PDAC tissues and pancreatic cancer cell lines, *HNF1B* was down-regulated compared with normal pancreatic tissues and this loss of expression contributed to disease aggressiveness.[62,80] Recently, a regulatory network analysis reported that *HNF1B*, among thousand transcription factors, was the top enriched gene expressed in the normal pancreatic tissue compared with the PDAC regulatory network, identifying HNF1B as a master regulator of PDAC and its subtypes.[82] The present study shows that loss of Hnf1b activity can induce pancreatitis, pancreatic neoplasia, and facilitates the onset of $Kras^{G12V}$-induced PanIN. We show here some molecular mechanisms that link *Hnf1b* dysfunction to pancreatic neoplasia and tumorigenesis. Understanding the first steps of pancreatic tumorigenesis is important and may provide new therapeutic strategies aimed at restoring a normal differentiated state. Hnf1b appears to act as a pancreatic tumor suppressor, which is important for the epithelial state maintenance. Hnf6, one downstream target of Hnf1b, also was proposed as a tumor suppressor,[61] suggesting that maintenance of the ductal phenotype could be important in cancer prevention. Defining the molecular mechanisms underlying the initiation of pancreatic cancer is highly relevant for the development of early detection markers and of potentially novel treatments. Insight on the role of Hnf1b in pancreatic cancer development could lead to its use as a biomarker for early detection and prognosis. Reinforcing HNF1B expression may represent a novel therapeutic strategy to improve the survival of patients with PDAC, together with restoring ciliogenesis by pharmacologic means to improve the effectiveness of other curative options. Thus, these new insights offer potential novel therapeutic strategies.

Material and Methods

Mouse Lines

The *Hnf1b* conditional knockout ($Hnf1b^{tm1Ics}$ denoted as $Hnf1b^{flox/flox}$) carrying LoxP sites flanking exon 4[13] and $Sox9\text{-}CreER^{T2}$[14] lines have been described previously. The $R26R^{YFP}$ line (B6.129X1-Gt[ROSA]26Sortm1[EYFP]Cos/J) from the Jackson Laboratory (Bar Harbor, ME) was used to assess recombination efficiency. We performed a conditional deletion of *Hnf1b* in pancreatic ducts by crossing the Hnf1b-floxed mouse line with the TM-inducible $Sox9\text{-}CreER^{T2}$ line to generate $Sox9\text{-}Cre^{ER};Hnf1b^{fl/fl}$ mice, referred to as *mutants*. $Hnf1b^{fl/+}$ or $Hnf1b^{fl/fl}$ mice are referred to as *controls*. Heterozygous $Sox9\text{-}CreER;Hnf1b^{+/fl}$ mice showed no phenotype (data not shown). The Elas-tTA; TetO-Flpase; FRT-Stop-FRT $Kras^{G12V}$ line expressed FLP recombinase under the control of the elastase promoter in a tet-off system, allowing selective expression of the KrasG12V oncoprotein in pancreatic acinar cells. Untreated mice developed PanIN lesions with a long latency[83] and were used in crossings with $Sox9\text{-}CreER;Hnf1b^{fl/fl}$ mutants with TM induction perinatally to assess if ductal Hnf1b inactivation promotes PanIN progression in concert with Kras activated in acinar cells. Elas-tTA; TetO-Flpase; $Kras^{G12V}$ are referred to as Kras and $Sox9\text{-}Cre^{ER};Hnf1b^{fl/fl}$;Elas-tTA; TetO-Flpase; $Kras^{G12V}$ are referred to as mutant;Kras. Animal experiments were conducted in accordance with French and European ethical legal guidelines and the local ethical committee for animal care (Comité d'Éthique en Expérimentation Animale Charles Darwin no. 5, approval number: 01508).

Tamoxifen Treatment

TM (T5648; Sigma-Aldrich, Lyon, France) was dissolved at 25 mg/mL in corn oil and administered intraperitoneally to mice at a dose of 7 mg/40 g of mouse. For postnatal inactivation, TM injections were performed on lactating females during 3 consecutive days after birth, with 1 injection per day (P1, P2, P3), allowing pups to receive TM through breast milk. Dissections were performed at P8, P25, 2 months, and 5 months. For adult inactivation, TM was injected during 4 consecutive days, with 1 injection per day, to 6- or 10-week-old mice.

Cerulein Treatment

Two weeks after adult *Hnf1b* inactivation with TM injections of 10-week-old mice, mice were injected with cerulein (C9026; Sigma), a decapeptide analogue of the pancreatic secretagogue cholecystokinin that induces acinar cell death, at a dose corresponding to 75 μg/kg. Cerulein was dissolved at 1 mg/mL in NaCl and administered to mice at 5 μL/g by injections intraperitoneally hourly, 7 times a day, for 2 consecutive days. Pancreata were harvested at 3 different times after the first cerulein injection: just before cerulein injection at D0, when acute pancreatitis was induced at D3, and when the pancreas was almost fully regenerated at D7.

Histology, Immunohistochemistry, and Immunofluorescence

Dissected pancreata were fixed in 4% formaldehyde overnight and embedded in paraffin. Sections (7-μm thick) were prepared, deparaffinized, and rehydrated for histologic staining. For H&E staining, slides were incubated with Harris solution (HHS16; Sigma) for 1 minute, and in eosin (HT110216; Sigma) for 3 minutes. For Masson's trichrome staining, slides were incubated with Harris for 5 minutes, rinsed with lithium carbonate and water, incubated with Fuchsin-Ponceau for 3 minutes, and then rinsed with acidified water and 1% phosphomolybdic acid. Slides then were stained with 1% light green for 20 minutes and rinsed with acidified water. For Alcian blue staining, slides were incubated with Alcian blue solution (pH 2.5) for 30 minutes, prepared with Alcian blue 8GX (A3157; Sigma) in 3% acetic acid, rinsed with water, and counterstained with Nuclear Fast Red (Sigma-Aldrich) solution for 5 minutes. Slides were dehydrated before mounting.

Sections were processed for immunofluorescence or immunohistochemistry using a previously described protocol.[16] Briefly, epitope retrieval was performed by heating

the slides in a microwave in citric acid buffer (10 mmol/L, pH 6). Permeabilization was performed in phosphate-buffered saline (PBS)/Triton X-100 (Sigma-Aldrich) 0.3%, and sections were incubated in blocking solution (10% milk, 1% bovine serum albumin, 0.1% 10× Triton X-100 in PBS 1× or 1.5% horse/goat serum in PBS 1×) before antibody staining. Nuclei were stained with 4′,6-diamidino-2-phenylindole (1/1000; Sigma) in the secondary antibody staining step. For signal amplification, we used a biotinylated anti-rabbit or anti-goat antibody before incubating with streptavidin–Alexa 594 or streptavidin–Alexa 488. Epitope retrieval for CTGF immunohistochemistry was performed by heating slides in a pressure cooker for 15 minutes. Slides then were incubated in 3% H_2O_2 before blocking to eliminate endogenous peroxidase activity. For all other immunohistochemistry experiments, slides were incubated in 1% H_2O_2/50% methanol solution before blocking to eliminate endogenous peroxidase activity. The Vectastain peroxidase ABC system (Vector, Peterborough, UK) was used for Sox9, F4/80, vimentin, CTGF, Hey2, Phospho-AKT, Phospho-SMAD, and claudin 18 immunostainings. Nuclei were counterstained with hematoxylin. Primary antibodies are listed in Table 1. Images were acquired using a Zeiss (Marly-le Roi, France) Axio Observer.Z1 microscope with apotome. For histology, immunofluorescence, and immunohistochemistry, at least 2 sections per pancreas and at least 3 different pancreases of each genotype were analyzed.

Quantification of Recombined GFP+ Ducts, Ciliated Ductal Cells, Duct Area, Proliferation and Apoptosis, and PanINs

Quantification of GFP+ ducts in mutants was performed with GFP/Hnf1b immunostainings. More than 2500 GFP+ cells and 500 Hnf1b+ cells were counted (n = 3).

Quantification of ciliated ductal cells at P8 was performed by counting Sox9+ cells with the cilium stained with acetylated tubulin. Almost 500 cells were counted for controls and more than 1000 cells were counted for mutants (control, n = 7; mutant, n = 11). Quantifications of Sox9+ and Amylase+ cells at P8 were performed with at least 2 sections per pancreas (control, n = 4; mutant, n = 4). More than 15,000 Sox9+ and 22,000 amylase+ cells were counted for each genotype. The numbers of Sox9+ and amylase+ cells per mm^2 were obtained by dividing the numbers of Sox9+ and amylase+ cells by the corresponding cross-sectional areas.

Proliferation of ductal and acinar cells was determined by immunolabeling with PPH3 and Sox9 or amylase antibodies, respectively. Positive cells were scored from at least 3 nonoverlapping fields for each section at 10× magnification. The percentages of PPH3-positive cells were calculated by dividing the number of ductal or acinar cells labeled with PPH3 by the total number of cells expressing Sox9 or amylase. Quantification was performed with at least 2 sections per pancreas (control, n = 4; mutant, n = 4).

Table 1. Antibodies

Antigen	Host	Dilution	Manufacturer
Amylase	Goat	1/50	sc-12821; Santa Cruz Biotechnology (Heidelberg, Germany)
Acetylated α-tubulin	Mouse	1/300	T6793; Sigma
AKT-phospho-S473	Mouse	1/100	66444-1-Ig; Proteintech (Manchester, UK)
Arl13b	Mouse	1/100	75-287; Antibodies, Inc (Davis, CA)
β-catenin	Mouse	1/100	610153; BD Biosciences (San Jose, CA)
Claudin 18	Rabbit	1/250	700178; ThermoFisher Scientific
CTGF	Rabbit	1/3000	AAS91519C; Antibody Verify (Las Vegas, NV)
F4/80	Rat	1/500	123102; BioLegend (San Diego, CA)
Fabp4	Rabbit	1/200	ab13979; Abcam (Paris, France)
GFP	Chicken	1/400	GFP-1020; Aves Labs (Paris, France)
Hey2	Rabbit	1/100	10597-1-AP; Proteintech
Hnf1b	Rabbit	1/50	sc-22840; Santa Cruz
Hnf6	Guinea pig	1/500	Frederic Lemaigre's laboratory
Muc1	Hamster	1/100	HM-1630-PO; ThermoFisher Scientific
α-smooth muscle actin	Mouse	1/50	C6198; Sigma
Pan-cytokeratin	Mouse	1/100	C1801; Sigma
Phospho-histone H3	Mouse	1/300	9706; Cell Signaling (Danvers, MA)
Phospho-SMAD2 (Ser435, Ser 467)	Rabbit	1/150	44-244G; ThermoFisher Scientific
Protein kinase C zeta	Rabbit	1/500	sc-216; Santa Cruz
Sox9	Rabbit	1/100	AB5535; Millipore (Molsheim, France)
SPP1/osteopontin	Goat	1/100	AF808; R&D Systems
Vimentin	Goat	1/100	sc-7557; Santa Cruz
YAP	Mouse	1/50	sc-101199; Santa Cruz

Table 2. qPCR Primers

Name	Forward sequence (5'-3')	Reverse sequence (5'-3')
Amylase	CTGGGTTGATATTGCCAAGG	TGCACCTTGTCACCATGTCT
Birc5	CTGATTTGGCCCAGTGTTTT	CAGGGGAGTGCTTTCTATGC
Ccl2	AGCTGTAGTTTTTGTCACCAAGC	GTGCTGAAGACCTTAGGGCA
Ccl5	CCTCACCATATGGCTCGGAC	ACGACTGCAAGATTGGAGCA
CD2	AGGATTCTGGAGAGGGTCTCA	TCGCCTCACACTTGAATGGT
CD19	GTCATTGCAAGGTCAGCAGTG	GGGTCAGTCATTCGCTTCCT
Ck19	ACCCTCCCGAGATTACAACC	TCTGAAGTCATCTGCAGCCA
Col1A1	ACCTCAAGATGTGCCACTC	TGCTCTCTCCAAACCAGAC
CPA	CAACCCCTGCTCAGAAACTTACC	TGGACTTGACCTCCACTTCAGA
CTGF	GCCAACCGCAAGATCGGAGTGT	ACGGCCCCATCCAGGCAA
CXCL10	GCTGCCGTCATTTTCTGC	TCTCACTGGCCCGTCATC
Cyclophilin A	CAGGTCCTGGCATCTTGTCC	TTGCTGGTCTTGCCATTCCT
Cyr61	TCTGTGAAGTGCGTCCTTGT	CTGGTTCTGGGGATTTCTTG
Cys1	AGAGGAGCTCATGGCGAGCATT	GCCTGTGGCACAGATGCCAAGA
E-Cad	GCAGTCCCGGCTTCAGTTCC	GCCGGCCAGTGCATCCTT
EGFR	GCAGGGAGTGCGTGGAGAAATG	GTTGTCTGGTCCCCTGCCTGTA
F4/80	CTTTGGCTATGGGCTTCCAGTC	GCAAGGAGGACAGAGTTTATCGTG
Hes1	CAAAGACGGCCTCTGAGCAC	CCTTCGCCTCTTCTCCATGAT
Hey2	AGCGCCCTTGTGAGGAAACGA	TGTAGCGTGCCCAGGGTAATTG
Hnf1a	GTGTAACTGCACAGGAGGCAAA	TTCTCACGTGTCCCAAGACCTA
Hnf1b	GGCCTACGACCGGCAAAAGA	GGGAGACCCCTCGTTGCAAA
Hnf6	CAAATCACCATCTCCCAGCAG	CAGACTCCTCCTCCTGGCATT
IL10	CAGAGCCACATGCTCCTAGA	TGTCCAGCTGGTCCTTTGTT
Jag1	TGCCCTCCAGGACATAGTGG	ACTCTCCCCATGGTGATGCA
LAMC2	ATTGGCTCCCAACCCAGCAGA	ACAGCTGCCATCACCTCGACA
Mist1	TGGGCCTCCAGATCTCACCAA	CGTCACATGTCAGGTTTCTCTGCT
Muc1	CTCTGGAAGACCCCAGCTCCAA	CCACGGAGCCTGACCTGAACT
N-Cad	GCTGACCACGCTCACTGCT	ATCTGCCCATTCACGGGGTCTA
Notch2	CCTGCCAGGTTTTGAAGGGA	GGGCAGTCGTCGATATTCCG
Nr5a2	CTGCTGGACTACACGGTTTGC	CTGCCTGCTTGCTGATTGC
P8/Nupr1	GAGAAGCTGCTGCCAATACC	GTGTGGTGTCTGTGGTCTGG
Pkd1	GCTGCATGCCAGTTCTTTTG	TTTTAAAGTGCAGAAGCCCCA
Pkhd1	TGCTCCTCAGGCAGGCAATCG	ACCTGTACCCTGGGGTGGCTT
PPARg	GATGGAAGACCACTCGCATT	AACCATTGGGTCAGCTCTTG
Prox1	CGCAGAAGGACTCTCTTTGTC	GATTGGGTGATAGCCCTTCAT
Ptf1a	TTCCTGAAGCACCTTTGACAGA	ACGGAGTTTCCTGGACAGAGT
Rbpj	GTTTTGGCGAGAGTTTGTGGAAGAT	TGGAGGCCGCTCACCAAACT
SMA	GACGCTGCTCCAGCTATGT	AGTTGGTGATGATGCCGTGT
Sox9	AAGCCGACTCCCCACATTCCTC	CGCCCCTCTCGCTTCAGATCAA
Spp1	CCCTCCCGGTGAAAGTGACTGA	GCACCAGCCATGTGGCTATAGG
TGF-b1	AGAGGTCACCCGCGTGCTAAT	GGGCACTGCTTCCCGAATGTC
Vimentin	GGGAGAAATTGCAGGAGGAG	ATTCCACTTTGCGTTCAAGG

Acinar cell apoptosis was determined with a TUNEL analysis, performed using an in situ cell death detection kit (Roche Diagnostics, Meylan, France) and followed by amylase immunostaining. Apoptosis was quantified by counting the number of labeled nuclei. The percentage of TUNEL-positive cells was calculated by dividing the number of TUNEL+/amylase+ cells by the total number of amylase+ acinar cells. Quantification was performed with 3 sections per pancreas (control, n = 4; mutant, n = 4). More than 100 TUNEL-stained acinar cells were counted in controls and more than 800 in mutants.

All counting was performed with Adobe Photoshop CS4 (San Jose, CA).

Quantification of the percentage of remaining acini, adipocytes, fibrosis/infiltrates, ADM, and PanIN was performed on histologic sections of mutant pancreata (n = 6) with

ImageJ (National Institutes of Health, Bethesda, MD) and Fiji software.

Quantification of the lesion surface in mutant;Kras compared with Kras and mutants was performed by measuring the surface of the lesions positive for Alcian blue divided by the total surface of the pancreatic area in μm^2. The results are given in percentages. Each image of the most representative section per sample was acquired by a macro-apotome Zeiss Axiozoomer and the surfaces were quantified by Zen software. The total number of lesions was counted on each image acquired by the macro-apotome for each sample and was normalized by the total surface of the pancreatic area. The results are given as the number of lesions per cm^2. The size of each lesion also was quantified in μm^2 (mutants, n = 5; Kras, n = 4; mutant;Kras, n = 3).

Values are shown as means + SEM.

RNA Extraction and RT-qPCR

Total RNA from adult pancreas was isolated using the RNeasy Mini-kit (Qiagen, Courtaboeuf, France) and reverse-transcribed using the Superscript RT II Kit with random hexamers (Invitrogen, ThermoFisher Scientific, Illkirch, France). qPCR was performed using a SYBR Green master mix (Eurobiogreen QPCR Mix, Hi-ROX; Eurobio, Courtaboeuf, France). Primer sequences are provided in Table 2. The method of relative quantification was used to calculate expression levels, normalized to cyclophilin A and relative to wild-type complementary DNA from E15.5 pancreata. Values are shown as means + SEM.

Statistical Analysis

Statistical significance was determined using the Student t test or the nonparametric Mann–Whitney U test when appropriate. Statistical analyses were performed with GraphPad Prism 6.0 (GraphPad Software, Inc, La Jolla, CA). Differences were considered significant at a P value less than .05 (NS, not significant; $^*P < .05$; $^{**}P < .01$; $^{***}P < .001$).

References

1. Pinho AV, Chantrill L, Rooman I. Chronic pancreatitis: a path to pancreatic cancer. Cancer Lett 2014; 345:203–209.
2. De La OJ-P, Emerson LL, Goodman JL, Froebe SC, Illum BE, Curtis AB, Murtaugh LC. Notch and Kras reprogram pancreatic acinar cells to ductal intraepithelial neoplasia. Proc Natl Acad Sci U S A 2008; 105:18907–18912.
3. Guerra C, Schuhmacher AJ, Cañamero M, Grippo PJ, Verdaguer L, Pérez-Gallego L, Dubus P, Sandgren EP, Barbacid M. Chronic pancreatitis is essential for induction of pancreatic ductal adenocarcinoma by K-Ras oncogenes in adult mice. Cancer Cell 2007; 11:291–302.
4. Kleeff J, Whitcomb DC, Shimosegawa T, Esposito I, Lerch MM, Gress T, Mayerle J, Drewes AM, Rebours V, Akisik F, Muñoz JED, Neoptolemos JP. Chronic pancreatitis. Nat Rev Dis Primers 2017;3:17060.
5. Reichert M, Rustgi AK. Pancreatic ductal cells in development, regeneration, and neoplasia. J Clin Invest 2011; 121:4572–4578.
6. Larsen HL, Grapin-Botton A. The molecular and morphogenetic basis of pancreas organogenesis. Semin Cell Dev Biol 2017;66:51–68.
7. Cano DA, Murcia NS, Pazour GJ, Hebrok M. Orpk mouse model of polycystic kidney disease reveals essential role of primary cilia in pancreatic tissue organization. Development 2004;131:3457–3467.
8. Cano DA, Sekine S, Hebrok M. Primary cilia deletion in pancreatic epithelial cells results in cyst formation and pancreatitis. Gastroenterology 2006;131:1856–1869.
9. Zhang Q, Davenport JR, Croyle MJ, Haycraft CJ, Yoder BK. Disruption of IFT results in both exocrine and endocrine abnormalities in the pancreas of Tg737(orpk) mutant mice. Lab Invest 2005;85:45–64.
10. Lodh S, O'Hare EA, Zaghloul NA. Primary cilia in pancreatic development and disease. Birth Defects Res C Embryo Today 2014;102:139–158.
11. Maestro MA, Boj SF, Luco RF, Pierreux CE, Cabedo J, Servitja JM, German MS, Rousseau GG, Lemaigre FP, Ferrer J. Hnf6 and Tcf2 (MODY5) are linked in a gene network operating in a precursor cell domain of the embryonic pancreas. Hum Mol Genet 2003; 12:3307–3314.
12. Solar M, Cardalda C, Houbracken I, Martín M, Maestro MA, De Medts N, Xu X, Grau V, Heimberg H, Bouwens L, Ferrer J. Pancreatic exocrine duct cells give rise to insulin-producing beta cells during embryogenesis but not after birth. Dev Cell 2009; 17:849–860.
13. De Vas MG, Kopp JL, Heliot C, Sander M, Cereghini S, Haumaitre C. Hnf1b controls pancreas morphogenesis and the generation of Ngn3+ endocrine progenitors. Development 2015;142:871–882.
14. Kopp JL, Dubois CL, Schaffer AE, Hao E, Shih HP, Seymour PA, Ma J, Sander M. Sox9+ ductal cells are multipotent progenitors throughout development but do not produce new endocrine cells in the normal or injured adult pancreas. Development 2011;138:653–665.
15. Houbracken I, Bouwens L. Acinar cells in the neonatal pancreas grow by self-duplication and not by neogenesis from duct cells. Sci Rep 2017;7:12643.
16. Haumaitre C, Barbacci E, Jenny M, Ott MO, Gradwohl G, Cereghini S. Lack of TCF2/vHNF1 in mice leads to pancreas agenesis. Proc Natl Acad Sci U S A 2005; 102:1490–1495.
17. Gresh L, Fischer E, Reimann A, Tanguy M, Garbay S, Shao X, Hiesberger T, Fiette L, Igarashi P, Yaniv M, Pontoglio M. A transcriptional network in polycystic kidney disease. EMBO J 2004;23:1657–1668.
18. Masyuk TV, Huang BQ, Ward CJ, Masyuk AI, Yuan D, Splinter PL, Punyashthiti R, Ritman EL, Torres VE, Harris PC, LaRusso NF. Defects in cholangiocyte fibrocystin expression and ciliary structure in the PCK rat. Gastroenterology 2003; 125:1303–1310.
19. Raynaud P, Tate J, Callens C, Cordi S, Vandersmissen P, Carpentier R, Sempoux C, Devuyst O, Pierreux CE,

Courtoy P, Dahan K, Delbecque K, Lepreux S, Pontoglio M, Guay-Woodford LM, Lemaigre FP. A classification of ductal plate malformations based on distinct pathogenic mechanisms of biliary dysmorphogenesis. Hepatology 2011;53:1959–1966.
20. Kilic G, Wang J, Sosa-Pineda B. Osteopontin is a novel marker of pancreatic ductal tissues and of undifferentiated pancreatic precursors in mice. Dev Dyn 2006; 235:1659–1667.
21. Westmoreland JJ, Kilic G, Sartain C, Sirma S, Blain J, Rehg J, Harvey N, Sosa-Pineda B. Pancreas-specific deletion of Prox1 affects development and disrupts homeostasis of the exocrine pancreas. Gastroenterology 2012;142:999–1009.e6.
22. Kobayashi T, Dynlacht BD. Regulating the transition from centriole to basal body. J Cell Biol 2011; 193:435–444.
23. Basten SG, Giles RH. Functional aspects of primary cilia in signaling, cell cycle and tumorigenesis. Cilia 2013; 2:6.
24. Jiang L, Sun L, Edwards G, Manley M Jr, Wallace DP, Septer S, Manohar C, Pritchard MT, Apte U. Increased YAP activation is associated with hepatic cyst epithelial cell proliferation in ARPKD/CHF. Gene Expr 2017; 17:313–326.
25. Halder G, Dupont S, Piccolo S. Transduction of mechanical and cytoskeletal cues by YAP and TAZ. Nat Rev Mol Cell Biol 2012;13:591–600.
26. Low BC, Pan CQ, Shivashankar GV, Bershadsky A, Sudol M, Sheetz M. YAP/TAZ as mechanosensors and mechanotransducers in regulating organ size and tumor growth. FEBS Lett 2014;588:2663–2670.
27. Panciera T, Azzolin L, Cordenonsi M, Piccolo S. Mechanobiology of YAP and TAZ in physiology and disease. Nat Rev Mol Cell Biol 2017;18:758–770.
28. Pi L, Robinson PM, Jorgensen M, Oh SH, Brown AR, Weinreb PH, Trinh TL, Yianni P, Liu C, Leask A, Violette SM, Scott EW, Schultz GS, Petersen BE. Connective tissue growth factor and integrin αvβ6: a new pair of regulators critical for ductular reaction and biliary fibrosis in mice. Hepatology 2015;61:678–691.
29. Liu F, Lagares D, Choi KM, Stopfer L, Marinković A, Vrbanac V, Probst CK, Hiemer SE, Sisson TH, Horowitz JC, Rosas IO, Fredenburgh LE, Feghali-Bostwick C, Varelas X, Tager AM, Tschumperlin DJ. Mechanosignaling through YAP and TAZ drives fibroblast activation and fibrosis. Am J Physiol Lung Cell Mol Physiol 2015;308:L344–L357.
30. Gao T, Zhou D, Yang C, Singh T, Penzo-Méndez A, Maddipati R, Tzatsos A, Bardeesy N, Avruch J, Stanger BZ. Hippo signaling regulates differentiation and maintenance in the exocrine pancreas. Gastroenterology 2013;144:1543–1553, 1553.e1.
31. Morvaridi S, Dhall D, Greene MI, Pandol SJ, Wang Q. Role of YAP and TAZ in pancreatic ductal adenocarcinoma and in stellate cells associated with cancer and chronic pancreatitis. Sci Rep 2015;5:16759.
32. Gruber R, Panayiotou R, Nye E, Spencer-Dene B, Stamp G, Behrens A. YAP1 and TAZ control pancreatic cancer initiation in mice by direct up-regulation of JAK–STAT3 signaling. Gastroenterology 2016; 151:526–539.
33. Means AL, Meszoely IM, Suzuki K, Miyamoto Y, Rustgi AK, Coffey RJ Jr, Wright CV, Stoffers DA, Leach SD. Pancreatic epithelial plasticity mediated by acinar cell transdifferentiation and generation of nestin-positive intermediates. Development 2005; 132:3767–3776.
34. Navas C, Hernández-Porras I, Schuhmacher AJ, Sibilia M, Guerra C, Barbacid M. EGF receptor signaling is essential for k-ras oncogene-driven pancreatic ductal adenocarcinoma. Cancer Cell 2012;22:318–330.
35. Liu J, Akanuma N, Liu C, Naji A, Halff GA, Washburn WK, Sun L, Wang P. TGF-β1 promotes acinar to ductal metaplasia of human pancreatic acinar cells. Sci Rep 2016;6:30904.
36. Prévot P-P, Simion A, Grimont A, Colletti M, Khalaileh A, Van den Steen G, Sempoux C, Xu X, Roelants V, Hald J, Bertrand L, Heimberg H, Konieczny SF, Dor Y, Lemaigre FP, Jacquemin P. Role of the ductal transcription factors HNF6 and Sox9 in pancreatic acinar-to-ductal metaplasia. Gut 2012;61:1723–1732.
37. Chuvin N, Vincent DF, Pommier RM, Alcaraz LB, Gout J, Caligaris C, Yacoub K, Cardot V, Roger E, Kaniewski B, Martel S, Cintas C, Goddard-Léon S, Colombe A, Valantin J, Gadot N, Servoz E, Morton J, Goddard I, Couvelard A, Rebours V, Guillermet J, Sansom OJ, Treilleux I, Valcourt U, Sentis S, Dubus P, Bartholin L. Acinar-to-ductal metaplasia induced by transforming growth factor beta facilitates KRASG12D-driven pancreatic tumorigenesis. Cell Mol Gastroenterol Hepatol 2017;4:263–282.
38. Miyamoto Y, Maitra A, Ghosh B, Zechner U, Argani P, Iacobuzio-Donahue CA, Sriuranpong V, Iso T, Meszoely IM, Wolfe MS, Hruban RH, Ball DW, Schmid RM, Leach SD. Notch mediates TGFα-induced changes in epithelial differentiation during pancreatic tumorigenesis. Cancer Cell 2003;3:565–576.
39. Lammert E, Brown J, Melton DA. Notch gene expression during pancreatic organogenesis. Mech Dev 2000; 94:199–203.
40. Bhanot U, Köhntop R, Hasel C, Möller P. Evidence of Notch pathway activation in the ectatic ducts of chronic pancreatitis. J Pathol 2008;214:312–319.
41. Mallo GV, Fiedler F, Calvo EL, Ortiz EM, Vasseur S, Keim V, Morisset J, Iovanna JL. Cloning and expression of the Rat p8 cDNA, a new gene activated in pancreas during the acute phase of pancreatitis, pancreatic development, and regeneration, and which promotes cellular growth. J Biol Chem 1997; 272:32360–32369.
42. Siersbaek R, Nielsen R, Mandrup S. PPARgamma in adipocyte differentiation and metabolism–novel insights from genome-wide studies. FEBS Lett 2010; 584:3242–3249.
43. Apte MV, Pirola RC, Wilson JS. Pancreatic stellate cells: a starring role in normal and diseased pancreas. Front Physiol 2012;3:344.
44. Korc M. Pancreatic cancer-associated stroma production. Am J Surg 2007;194:S84–S86.

45. Haque I, Mehta S, Majumder M, Dhar K, De A, McGregor D, Van Veldhuizen PJ, Banerjee SK, Banerjee S. Cyr61/CCN1 signaling is critical for epithelial-mesenchymal transition and stemness and promotes pancreatic carcinogenesis. Mol Cancer 2011; 10:8.
46. Leach SD. Epithelial differentiation in pancreatic development and neoplasia: new niches for nestin and Notch. J Clin Gastroenterol 2005;39:S78–S82.
47. Criscimanna A, Speicher JA, Houshmand G, Shiota C, Prasadan K, Ji B, Logsdon CD, Gittes GK, Esni F. Duct cells contribute to regeneration of endocrine and acinar cells following pancreatic damage in adult mice. Gastroenterology 2011;141:1451–1462, 1462.e1–6.
48. Murtaugh LC, Keefe MD. Regeneration and repair of the exocrine pancreas. Annu Rev Physiol 2015;77:229–249.
49. Zhang M-Z, Mai W, Li C, Cho SY, Hao C, Moeckel G, Zhao R, Kim I, Wang J, Xiong H, Wang H, Sato Y, Wu Y, Nakanuma Y, Lilova M, Pei Y, Harris RC, Li S, Coffey RJ, Sun L, Wu D, Chen XZ, Breyer MD, Zhao ZJ, McKanna JA, Wu G. PKHD1 protein encoded by the gene for autosomal recessive polycystic kidney disease associates with basal bodies and primary cilia in renal epithelial cells. PNAS 2004;101:2311–2316.
50. Kim I, Fu Y, Hui K, Moeckel G, Mai W, Li C, Liang D, Zhao P, Ma J, Chen XZ, George AL Jr, Coffey RJ, Feng ZP, Wu G. Fibrocystin/polyductin modulates renal tubular formation by regulating polycystin-2 expression and function. J Am Soc Nephrol 2008; 19:455–468.
51. Dong F, Chen Q-Q, Zhuang Z-H, He QL, Wang FQ, Liu QC, Liu HK, Wang Y. Multiple gene mutations in patients with type 2 autoimmune pancreatitis and its clinical features. Cent Eur J Immunol 2014;39:77–82.
52. Hou X, Mrug M, Yoder BK, Lefkowitz EJ, Kremmidiotis G, D'Eustachio P, Beier DR, Guay-Woodford LM. Cystin, a novel cilia-associated protein, is disrupted in the cpk mouse model of polycystic kidney disease. J Clin Invest 2002;109:533–540.
53. Pazour GJ, Dickert BL, Vucica Y, Seeley ES, Rosenbaum JL, Witman GB, Cole DG. Chlamydomonas IFT88 and its mouse homologue, polycystic kidney disease gene tg737, are required for assembly of cilia and flagella. J Cell Biol 2000;151:709–718.
54. Oh EC, Katsanis N. Cilia in vertebrate development and disease. Development 2012;139:443–448.
55. Pugacheva EN, Jablonski SA, Hartman TR, Henske EP, Golemis EA. HEF1-dependent Aurora A activation induces disassembly of the primary cilium. Cell 2007; 129:1351–1363.
56. Pierreux CE, Poll AV, Kemp CR, Clotman F, Maestro MA, Cordi S, Ferrer J, Leyns L, Rousseau GG, Lemaigre FP. The transcription factor hepatocyte nuclear factor-6 controls the development of pancreatic ducts in the mouse. Gastroenterology 2006;130:532–541.
57. Zhang H, Ables ET, Pope CF, Washington MK, Hipkens S, Means AL, Path G, Seufert J, Costa RH, Leiter AB, Magnuson MA, Gannon M. Multiple, temporal-specific roles for HNF6 in pancreatic endocrine and ductal differentiation. Mech Dev 2009;126:958–973.
58. Augereau C, Collet L, Vargiu P, Guerra C, Ortega S, Lemaigre FP, Jacquemin P. Chronic pancreatitis and lipomatosis are associated with defective function of ciliary genes in pancreatic ductal cells. Hum Mol Genet 2016;22:5017–5026.
59. Badano JL, Mitsuma N, Beales PL, Katsanis N. The ciliopathies: an emerging class of human genetic disorders. Annu Rev Genomics Hum Genet 2006;7:125–148.
60. Jiang X, Zhang W, Kayed H, Zheng P, Giese NA, Friess H, Kleeff J. Loss of ONECUT1 expression in human pancreatic cancer cells. Oncol Rep 2008; 19:157–163.
61. Pekala KR, Ma X, Kropp PA, Petersen CP1, Hudgens CW, Chung CH, Shi C, Merchant NB, Maitra A, Means AL, Gannon MA. Loss of HNF6 expression correlates with human pancreatic cancer progression. Lab Invest 2014;94:517–527.
62. Drosos Y, Neale G, Ye J, Paul L, Kuliyev E, Maitra A, Means AL, Washington MK, Rehg J, Finkelstein DB, Sosa-Pineda B. Prox1-heterozygosis sensitizes the pancreas to oncogenic Kras-induced neoplastic transformation. Neoplasia 2016;18:172–184.
63. Seeley ES, Carrière C, Goetze T, Longnecker DS, Korc M. Pancreatic cancer and precursor pancreatic intraepithelial neoplasia lesions are devoid of primary cilia. Cancer Res 2009;69:422–430.
64. Zhao B, Tumaneng K, Guan K-L. The Hippo pathway in organ size control, tissue regeneration and stem cell self-renewal. Nat Cell Biol 2011;13:877–883.
65. di Mola FF, Friess H, Martignoni ME, Di Sebastiano P, Zimmermann A, Innocenti P, Graber H, Gold LI, Korc M, Büchler MW. Connective tissue growth factor is a regulator for fibrosis in human chronic pancreatitis. Ann Surg 1999;230:63–71.
66. Charrier A, Brigstock DR. Regulation of pancreatic function by connective tissue growth factor (CTGF, CCN2). Cytokine Growth Factor Rev 2013;24:59–68.
67. Kosanam H, Prassas I, Chrystoja CC, Soleas I, Chan A, Dimitromanolakis A, Blasutig IM, Rückert F, Gruetzmann R, Pilarsky C, Maekawa M, Brand R, Diamandis EP. Laminin, gamma 2 (LAMC2): a promising new putative pancreatic cancer biomarker identified by proteomic analysis of pancreatic adenocarcinoma tissues. Mol Cell Proteomics 2013; 12:2820–2832.
68. Rovira M, Scott S-G, Liss AS, Jensen J, Thayer SP, Leach SD. Isolation and characterization of centroacinar/terminal ductal progenitor cells in adult mouse pancreas. Proc Natl Acad Sci U S A 2010;107:75–80.
69. Mazur PK, Einwächter H, Lee M, Sipos B, Nakhai H, Rad R, Zimber-Strobl U, Strobl LJ, Radtke F, Klöppel G, Schmid RM, Siveke JT. Notch2 is required for progression of pancreatic intraepithelial neoplasia and development of pancreatic ductal adenocarcinoma. Proc Natl Acad Sci U S A 2010;107: 13438–13443.
70. Friess H, Lu Z, Riesle E, Uhl W, Bründler AM, Horvath L, Gold LI, Korc M, Büchler MW. Enhanced expression of TGF-betas and their receptors in human acute pancreatitis. Ann Surg 1998;227:95–104.

71. Stanger BZ, Hebrok M. Control of cell identity in pancreas development and regeneration. Gastroenterology 2013;144:1170–1179.
72. Lugea A, Nan L, French SW, Bezerra JA, Gukovskaya AS, Pandol SJ. Pancreas recovery following cerulein-induced pancreatitis is impaired in plasminogen-deficient mice. Gastroenterology 2006; 131:885–899.
73. Chen Y-Z, Gao Q, Zhao X-Z, Chen YZ, Bennett CL, Xiong XS, Mei CL, Shi YQ, Chen XM. Systematic review of TCF2 anomalies in renal cysts and diabetes syndrome/maturity onset diabetes of the young type 5. Chin Med J 2010;123:3326–3333.
74. Grisanzio C, Werner L, Takeda D, Awoyemi BC, Pomerantz MM, Yamada H, Sooriakumaran P, Robinson BD, Leung R, Schinzel AC, Mills I, Ross-Adams H, Neal DE, Kido M, Yamamoto T, Petrozziello G, Stack EC, Lis R, Kantoff PW, Loda M, Sartor O, Egawa S, Tewari AK, Hahn WC, Freedman ML. Genetic and functional analyses implicate the NUDT11, HNF1B, and SLC22A3 genes in prostate cancer pathogenesis. Proc Natl Acad Sci U S A 2012;109:11252–11257.
75. Cuff J, Salari K, Clarke N, Esheba GE, Forster AD, Huang S, West RB, Higgins JP, Longacre TA, Pollack JR. Integrative bioinformatics links HNF1B with clear cell carcinoma and tumor-associated thrombosis. PLoS One 2013;8:e74562.
76. Buchner A, Castro M, Hennig A, Popp T, Assmann G, Stief CG, Zimmermann W. Downregulation of HNF-1B in renal cell carcinoma is associated with tumor progression and poor prognosis. Urology 2010;76:507. e6–11.
77. Terasawa K, Toyota M, Sagae S, Ogi K, Suzuki H, Sonoda T, Akino K, Maruyama R, Nishikawa N, Imai K, Shinomura Y, Saito T, Tokino T. Epigenetic inactivation of TCF2 in ovarian cancer and various cancer cell lines. Br J Cancer 2006;94:914–921.
78. Silva TD, Vidigal VM, Felipe AV, DE Lima JM, Neto RA, Saad SS, Forones NM. DNA methylation as an epigenetic biomarker in colorectal cancer. Oncol Lett 2013; 6:1687–1692.
79. Li D, Duell EJ, Yu K, Risch HA, Olson SH, Kooperberg C, Wolpin BM, Jiao L, Dong X, Wheeler B, Arslan AA, Bueno-de-Mesquita HB, Fuchs CS, Gallinger S, Gross M, Hartge P, Hoover RN, Holly EA, Jacobs EJ, Klein AP, LaCroix A, Mandelson MT, Petersen G, Zheng W, Agalliu I, Albanes D, Boutron-Ruault MC, Bracci PM, Buring JE, Canzian F, Chang K, Chanock SJ, Cotterchio M, Gaziano JM, Giovannucci EL, Goggins M, Hallmans G, Hankinson SE, Hoffman Bolton JA, Hunter DJ, Hutchinson A, Jacobs KB, Jenab M, Khaw KT, Kraft P, Krogh V, Kurtz RC, McWilliams RR, Mendelsohn JB, Patel AV, Rabe KG, Riboli E, Shu XO, Tjønneland A, Tobias GS, Trichopoulos D, Virtamo J, Visvanathan K, Watters J, Yu H, Zeleniuch-Jacquotte A, Amundadottir L, Stolzenberg-Solomon RZ. Pathway analysis of genome-wide association study data highlights pancreatic development genes as susceptibility factors for pancreatic cancer. Carcinogenesis 2012; 33:1384–1390.
80. Hoskins JW, Jia J, Flandez M, Parikh H, Xiao W, Collins I, Emmanuel MA, Ibrahim A, Powell J, Zhang L, Malats N, Bamlet WR, Petersen GM, Real FX, Amundadottir LT. Transcriptome analysis of pancreatic cancer reveals a tumor suppressor function for HNF1A. Carcinogenesis 2014;35:2670–2678.
81. Klein AP, Wolpin BM, Risch HA, Stolzenberg-Solomon RZ, Mocci E, Zhang M, Canzian F, Childs EJ, Hoskins JW, Jermusyk A, Zhong J, Chen F, Albanes D, Andreotti G, Arslan AA, Babic A, Bamlet WR, Beane-Freeman L, Berndt SI, Blackford A, Borges M, Borgida A, Bracci PM, Brais L, Brennan P, Brenner H, Bueno-de-Mesquita B, Buring J, Campa D, Capurso G, Cavestro GM, Chaffee KG, Chung CC, Cleary S, Cotterchio M, Dijk F, Duell EJ, Foretova L, Fuchs C, Funel N, Gallinger S, M Gaziano JM, Gazouli M, Giles GG, Giovannucci E, Goggins M, Goodman GE, Goodman PJ, Hackert T, Haiman C, Hartge P, Hasan M, Hegyi P, Helzlsouer KJ, Herman J, Holcatova I, Holly EA, Hoover R, Hung RJ, Jacobs EJ, Jamroziak K, Janout V, Kaaks R, Khaw KT, Klein EA, Kogevinas M, Kooperberg C, Kulke MH, Kupcinskas J, Kurtz RJ, Laheru D, Landi S, Lawlor RT, Lee IM, LeMarchand L, Lu L, Malats N, Mambrini A, Mannisto S, Milne RL, Mohelníková-Duchoňová B, Neale RE, Neoptolemos JP, Oberg AL, Olson SH, Orlow I, Pasquali C, Patel AV, Peters U, Pezzilli R, Porta M, Real FX, Rothman N, Scelo G, Sesso HD, Severi G, Shu XO, Silverman D, Smith JP, Soucek P, Sund M, Talar-Wojnarowska R, Tavano F, Thornquist MD, Tobias GS, Van Den Eeden SK, Vashist Y, Visvanathan K, Vodicka P, Wactawski-Wende J, Wang Z, Wentzensen N, White E, Yu H, Yu K, Zeleniuch-Jacquotte A, Zheng W, Kraft P, Li D, Chanock S, Obazee O, Petersen GM, Amundadottir LT. Genome-wide meta-analysis identifies five new susceptibility loci for pancreatic cancer. Nat Commun 2018;9:556.
82. Janky R, Binda MM, Allemeersch J, Van den Broeck A, Govaere O, Swinnen JV, Roskams T, Aerts S, Topal B. Prognostic relevance of molecular subtypes and master regulators in pancreatic ductal adenocarcinoma. BMC Cancer 2016;16:632.
83. Blasco MT, Navas C, Martín-Serrano G, Graña-Castro O, Lechuga CG, Martín-Díaz L, Djurec M, Li J, Morales-Cacho L, Esteban-Burgos L, Perales-Patón J, Bousquet-Mur E, Castellano E, Jacob HKC, Cabras L, Musteanu M, Drosten M, Ortega S, Mulero F, Sainz B Jr, Dusetti N, Iovanna J, Sánchez-Bueno F, Hidalgo M, Khiabanian H, Rabadán R, Al-Shahrour F, Guerra C, Barbacid M. Complete regression of advanced pancreatic ductal adenocarcinomas upon combined inhibition of EGFR and C-RAF. Cancer Cell 2019;35:573–587.e6.

Received April 12, 2018. Accepted June 13, 2019.

Correspondence
Address correspondence to: Cecile Haumaitre, PhD, Sorbonne Université, Centre National de la Recherche Scientifique, Institut de Biologie Paris-Seine, 9 Quai Saint-Bernard, Batiment C-7eme Etage-Case 24, 75252 Paris Cedex 05, France. e-mail: cecile.haumaitre@inserm.fr; fax: (33) 1-44-27-34-45.

Acknowledgments
Thassadite Dirami and Aline Stedman contributed equally to this work. The authors thank Edouard Manzoni and Edwige Declerc for technical help, the

mouse facilities of the Unité mixte de Recherche UMR7622 - Institut de Biologie Paris-Seine for animal care, the imaging platform of the IBPS for image acquisitions with the macro-apotome, and Sophie Gournet for illustrations. The authors also thank P. Jacquemin and F. Lemaigre (De Duve Institute, Belgium) for the Hnf6 antibody, and Christine Vesque for critical reading of the manuscript.

Author contributions

Evans Quilichini, Mélanie Fabre, Thassadite Dirami, Aline Stedman, Matias De Vas, Ozge Ozguc, Raymond C. Pasek, Lucie Morillon, and Cécile Haumaitre performed experiments; Evans Quilichini, Thassadite Dirami, Aline Stedman, Matias De Vas, Ozge Ozguc, Lucie Morillon, Anne Couvelard, and Cécile Haumaitre analyzed and interpreted the data; Silvia Cereghini, Carmen Guerra, and Maureen Gannon provided materials; Cécile Haumaitre wrote the manuscript; Evans Quilichini, Aline Stedman, Matias De Vas, Raymond C. Pasek, Silvia Cereghini, Carmen Guerra, Anne Couvelard, and Maureen Gannon revised the manuscript; and Cécile Haumaitre designed and supervised the study and obtained funding.

Conflicts of interest

The authors disclose no conflicts.

Funding

Supported by the Centre National de la Recherche Scientifique, the Université Pierre et Marie Curie-Sorbonne Université, the Gefluc-Les Entreprises Contre le Cancer, the Societe Francophone du Diabete-Ypsomed, and Emergence Université Pierre et Marie Curie (C.H.); supported by a PhD fellowship from the French Ministère de la Recherche et de la Technologie (E.Q). Mélanie Fabre is an assistant engineer of the Centre National de la Recherche Scientifique. Also supported by Sorbonne Université (T.D. and A.S.); a PhD student fellowship from the European Marie Curie Initial Training Network-Biology of Liver and Pancreatic Development and Disease (M.D.V.); by a Master 1 fellowship (O.O.); by postdoctoral fellowship 14POST20380262 from the American Heart Association (R.C.P.); by the National Institutes of Health (U01 DK089540), and by grant 1-2011-592 from the Juvenile Diabetes Research Foundation (M.G.). Cécile Haumaitre is a permanent senior researcher of the Institut National de la Santé et de la Recherche Médicale.